

# Coalescing binary systems of compact objects: dynamics of angular momenta

Carlo Del Noce<sup>1</sup>, Giovanni Preti<sup>2</sup>, and Fernando de Felice<sup>3</sup>  
 Dipartimento di Fisica “G. Galilei”, Università di Padova,  
 Via Marzolo 8, 35131, Padova, Italy,  
 and INFN, Sezione di Padova

## ABSTRACT

The end state of a coalescing binary of compact objects depends strongly on the final total mass  $M$  and angular momentum  $J$ . Since gravitational radiation emission causes a slow evolution of the binary system through quasi-circular orbits down to the innermost stable one, in this paper we examine the corresponding behavior of the ratio  $J/M^2$  which must be less than  $1(G/c)$  or about  $0.7(G/c)$  for the formation of a black hole or a neutron star respectively. The results show cases for which, at the end of the inspiral phase, these conditions are not satisfied. The inclusion of spin effects leads us to a study of precession equations valid also for the calculation of gravitational waveforms.

**PACS number(s):** 04.25.Nx, 04.30.Db, 97.80.Fk, 97.60.Jd, 97.60.Lf.

**Subject headings:** binaries: close — gravitation

## 1. Introduction.

Binary systems of compact objects like neutron stars or black holes are promising sources of gravitational radiation (Thorne 1987; Schutz 1996); in fact at coalescence they emit a great amount of energy in the frequency range of LIGO and VIRGO detectors (Abramovici et al. 1992). At least a half of the observable stars come in binary or multiple systems (Batten 1973) and a significant fraction of these may evolve to neutron star or black hole binaries which would coalesce, due to gravitational wave emission, in a time less than

---

<sup>1</sup>delnoce@pd.infn.it

<sup>2</sup>preti@pd.infn.it

<sup>3</sup>defelice@pd.infn.it

the age of the universe. Moreover, recent estimates (Thorne 1987; Schutz 1986; Narayan, Piran, & Shemi 1991; Phinney 1991; Tutukov & Yungelson 1993; Yamaoka, Shigeyama, & Nomoto 1993) make us confident that a few coalescences of compact binaries per year could be seen within a distance of about 100 Mpc.

In order to extract signal from noise, an extremely precise theoretical prediction is needed for the gravitational waveform (Kidder 1995). Therefore much work was recently devoted to understand the evolution of the system (Kidder 1995; Damour 1987; Lincoln & Will 1990; Kidder, Will, & Wiseman 1993; Apostolatos et al. 1994; Blanchet, Damour, & Iyer 1995, Blanchet 1996; Will & Wiseman 1996; and references therein).

An open question concerns the body coming out of coalescence. It is well known that a stationary black hole of mass  $M$  and angular momentum  $J$  must satisfy the condition  $J/M^2 < 1(G/c)$ . Also for a neutron star the ratio  $cJ/(GM^2)$ , hereafter defined as “Kerr parameter”, is less than about 0.7 (Cook, Shapiro, & Teukolsky 1994; Friedman & Ipser 1992; Salgado et al. 1994a, 1994b), thus it is important to know how this ratio behaves during coalescence to see whether a black hole or a neutron star may actually result.

We also study the precession equations that describe the evolution of the bodies’ spins. Spin precession plays an important role in the physics of angular momentum, and its detailed knowledge is necessary for a consistent calculation of  $J/M^2$ . Moreover spin precession is very important for the modulation of the gravitational wave (Apostolatos et al. 1994; Kidder 1995; Cutler & Flanagan 1994). Our results in this study apply directly to this field.

The coalescence of a binary system consists of two phases. The first phase is a slow adiabatic inspiral of the orbits in which the energy and angular momentum loss are assumed to be driven only by emission of gravitational waves. The second phase is highly dynamical: interactions between the bodies involve their internal structure and full general relativistic effects must be taken into account.

In this paper we consider only the first phase with the purpose of determining the value of the Kerr parameter at the end of it, which is the initial value of the Kerr parameter for the following phase of evolution in dynamical time. This late-time evolution is not yet well understood, because its study is a formidable problem that can be attacked almost only by recourse to numerical methods. It is essential for this task to know what the choice of initial values can be (Cook 1994), and this paper is aimed as a help in understanding the state of the system in that critical moment of transition between the two phases.

We adopt the post-Newtonian formalism, which corresponds to a series expansion of all quantities in the parameter  $v/c$  assumed to be small. There are available in literature

formulae for all physical quantities pertaining to the physical system, which are valid through second post-Newtonian relative order, i.e., including terms of order  $(v/c)^4$  beyond the first nonzero one, and including spin effects (Kidder 1995). This should be a pretty good approximation throughout the inspiral phase up to the innermost stable circular orbit (ISCO) (Junker & Schäfer 1992).

We shall neglect properties of the gravitating bodies connected with their internal structure except their spins: no correction terms for tidal interactions will be included since they would be equivalent to post-Newtonian corrections of higher order than what here wanted (Lai & Wiseman 1996). Again this approximation is less justified for compact bodies only when their separation becomes comparable to the ISCO radius.

Our calculations refer to quasi-circular orbits, for it has been proved (Peters 1964; Lincoln & Will 1990) that all compact binaries have time enough to evolve toward quasi-circular orbits before coalescence, except those that are captured at near separations in highly eccentric orbits.

In §2 we consider the case of nonspinning bodies and examine the behavior of the corresponding Kerr parameter. In §3 this analysis is extended to spinning bodies; in this case, however, it is essential to take into account the time evolution of the relative orientations of the orbital and intrinsic angular momenta. Therefore §3.1 is focused on this topic. Section 3.2 then gives the results of the analysis of the Kerr parameter when spin precession effects are included. Our conclusions are drawn in §4. We devote an Appendix to the study of the precession equations, due to their interest both for the problem at hand and more generally for the study of the gravitational waveform, and provide analytical solutions for particular cases.

### 1.1. Conventions and Units.

Although we use measurement units in which the constant of light speed in vacuo  $c$  and the gravitational constant  $G$  appear explicitly, we shall always make an effort to work with dimensionless physically meaningful variables.

We refer to a system of coordinates that satisfy the harmonic condition, as usual in most related literature, and whose center of mass is fixed by the same “spin supplementary condition” (SSC) used in (Kidder 1995), that is the covariant SSC expressed by equation (A2a) in that reference.

We shall denote the “Schwarzschild masses” (Damour 1987) of the two bodies by  $m_1$

and  $m_2$ , their sum by  $m = m_1 + m_2$  and the system's reduced mass by  $\mu = m_1 m_2 / (m_1 + m_2)$ , then set  $\eta = \mu/m$ . Following Blanchet, Damour, & Iyer (1995) we define  $X_1 = m_1/m$ ,  $X_2 = m_2/m$  and notice that, since  $X_1 + X_2 = 1$  and  $X_1 X_2 = \eta$ ,  $X_1$  and  $X_2$  are functions of  $\eta$  only: namely,  $X_1 = \frac{1}{2} \pm (\frac{1}{4} - \eta)^{1/2}$ ,  $X_2 = \frac{1}{2} \mp (\frac{1}{4} - \eta)^{1/2}$ .

Moreover let  $\mathbf{x} = \mathbf{x}_1 - \mathbf{x}_2$  be the separation vector between the two bodies in the chosen coordinate frame,  $r = |\mathbf{x}|$ ,  $\mathbf{v} = d\mathbf{x}/dt$ ,  $\rho = (c^2/G) r/m$ ,  $\gamma = (G/c^2) m/r = 1/\rho$ ,  $\mathbf{L}_N = \mu(\mathbf{x} \times \mathbf{v})$ ,  $\hat{\mathbf{L}}_N = \mathbf{L}_N/|\mathbf{L}_N|$ ,  $\mathbf{L} = \mathbf{L}_N + \text{post-Newtonian corrections}$ , let  $E$  be the system's Noetherian energy (Damour 1987),  $M = m + E/c^2$ , and let  $\mathbf{J}$  be the system's Noetherian total angular momentum (Damour 1987),  $J = |\mathbf{J}|$ . We let  $\mathbf{S}_i$  be the spin angular momentum of the  $i$ th body,  $S_i = |\mathbf{S}_i|$ ,  $\hat{\mathbf{s}}_i = \mathbf{S}_i/S_i$  and  $\boldsymbol{\sigma}_i = (c/G) \mathbf{S}_i/m^2$  ( $i = 1, 2$ ). We write  $\chi_i X_i^2 = \sigma_i = |\boldsymbol{\sigma}_i|$ , so that  $\chi_i$  is the absolute value of the  $i$ th body's spin in units of  $(G/c) m_i^2$  or Kerr parameter, and ranges from 0 to 1 for a (Kerr) black hole and from 0 to about 0.7 for a neutron star (Friedman & Ipser 1992; Salgado et al. 1994a, 1994b). For purposes of later convenience in writing long equations we also define  $f = \hat{\mathbf{L}}_N \cdot \hat{\mathbf{s}}_1$ ,  $g = \hat{\mathbf{L}}_N \cdot \hat{\mathbf{s}}_2$ ,  $h = \hat{\mathbf{s}}_1 \cdot \hat{\mathbf{s}}_2$ ,  $V = \hat{\mathbf{L}}_N \cdot \hat{\mathbf{s}}_1 \times \hat{\mathbf{s}}_2$ .

## 2. Nonspinning bodies.

As stated in the introduction, we assume here that the evolution of a close binary of compact objects can be approximately described by an adiabatic inspiral of pointlike masses through quasi-circular orbits, when the bodies' separation is large compared to their sizes (Lincoln & Will 1990). The total mass of the system is given for both spinning and nonspinning bodies and to the order relevant for our purposes by the following expression (Wagoner & Will 1976; Junker & Schäfer 1992):

$$M = m \left[ 1 - \frac{\eta}{2} \gamma + \frac{\eta}{8} (7 - \eta) \gamma^2 + O(\gamma^{5/2}) \right]. \quad (1)$$

In the case of nonspinning bodies ( $S_1 = S_2 = 0$ ) the general formula for  $\mathbf{J}$  (Kidder 1995) reduces to

$$\mathbf{J} = \mu (Gmr)^{1/2} \hat{\mathbf{L}}_N \left[ 1 + 2\gamma + \frac{1}{2} (5 - 9\eta) \gamma^2 + O(\gamma^{5/2}) \right].$$

Since we have assumed an adiabatic evolution of the system along the sequence of quasi-circular orbits, up to the innermost stable one at  $r_{\text{ISCO}} \approx 6Gm/c^2$ , the actual expressions of the mass and angular momentum loss rate due to gravitational radiation emission are not essential to evaluate the behavior of  $M$  and  $\mathbf{J}$ . We can then study directly

the behavior of the Kerr parameter. We obtain:

$$\frac{c}{G} \frac{J}{M^2} = \eta \rho^{1/2} \left[ 1 + (2 + \eta)\gamma + \frac{1}{4} (10 - 17\eta + 4\eta^2) \gamma^2 + O(\gamma^{5/2}) \right]. \quad (2)$$

Since  $\eta$  ranges between 0 and  $\frac{1}{4}$ , the latter corresponding to a system of two bodies with equal masses, any deviation from equipartition of masses in the binary system would decrease the Kerr parameter.

Figure 1 is a contour plot of  $cJ/(GM^2)$  in the  $(\rho, \eta)$ -plane.

The approximation  $S_1 = S_2 = 0$  is good for the description of systems consisting of two slowly spinning neutron stars, since the common values of their Kerr parameters are less or much less than  $10^{-2}$  (de Felice & Yunqiang 1982). We notice that any process of slow energy and angular momentum dissipation that keeps the system in quasi-circular orbits decreases the Kerr parameter below unity just at the limit of validity of our approach ( $\rho \approx 6$ ). At this separation the conditions for the formation of a stationary rotating neutron star are hardly met; first because  $J/M^2 < 0.7(G/c)$  holds only if  $\eta$  is less than about 0.2, which corresponds to a more massive body about 2.6 times as large as the other, and this is not the case for a system consisting initially of neutron stars, second because the total mass  $M$  must be less than the limiting mass of neutron stars. Thus we conclude from an inspection of Figure 1 that, since the most probable case for a neutron star binary is that they have nearly equal masses, the outcome of a final coalescence could be either a fast rotating black hole or a highly rotationally excited neutron star.

### 2.1. Estimate of accuracy.

It is not at all straightforward to estimate the accuracy of equation (2) for all choices of  $\eta$  and all values of  $\rho$ . In order to perform a rigorous estimate we should either know something about the convergence of the post-Newtonian series (eq. [2]) or be able to solve the problem exactly. Instead our information on the post-Newtonian series is rather poor. We neither have an upper bound for the series remainder nor know anything about the first neglected terms. In fact we exploited all the information in our hands—that is the post-Newtonian terms known up to date—for our calculations. Moreover there are hints of slow convergence of post-Newtonian series, reported by some recent studies (Poisson 1995; Simone et al. 1997). If we assume that the largest error source in truncating the series is given by the first neglected term, we can take the term of order  $\gamma^{5/2}$  in brackets in equation (2) as the relative error, or better, as its order of magnitude. Moreover, we shall assume that the coefficient of the term  $\gamma^{5/2}$  is 1, a simplification possible because our units are such

that all coefficients in the post-Newtonian series are of order 1. Some values for the relative error thus estimated are given below:

$$\begin{array}{ll} \text{error} \approx 3 \cdot 10^{-8}, & \text{at } \rho = 10^3, \\ \text{error} \approx 10^{-5}, & \text{at } \rho = 10^2, \\ \text{error} \approx 0.11, & \text{at } \rho = 6. \end{array}$$

Our confidence in the above estimate may be strengthened by a comparison with the case of a test mass in circular orbit around a Schwarzschild black hole. This problem of a test mass and a Schwarzschild black hole is well known and exactly solved. Actually it provides almost a benchmark for all post-Newtonian calculations, since agreement in the limit of  $\eta$  going to zero gives a necessary condition for their validity. We might also conjecture (Kidder, Will, & Wiseman 1993) that this comparison gives a pessimistic estimate of the error, since the post-Newtonian series is poorly convergent in the Schwarzschild case. The formula analogous to equation (2) for a test mass in circular orbit around a black hole reads

$$\frac{c}{G} \frac{J}{M^2} = \eta \rho^{1/2} \frac{\sqrt{(1+\gamma)^2/(1-2\gamma)}}{\left\{1 + \eta \sqrt{(1-\gamma)^2/[(1+\gamma)(1-2\gamma)]}\right\}^2}.$$

Since both equation (2) and the above equation are 0 when  $\eta$  is 0, we actually shall divide them by  $\eta$ , before any comparison. Thus the second post-Newtonian development of the above formula coincides with equation (2) at  $\eta = 0$ . The difference between the two formulae—which is a rigorous estimate of the post-Newtonian terms neglected in equation (2) in the limit  $\eta = 0$ —is very small, being less than  $10^{-3}$  for  $\rho \gtrsim 28.3$ , and showing a sudden increase for decreasing  $\rho$  only at  $\rho \lesssim 16$  (due to Schwarzschild behavior) but keeping anyway below  $6.4 \times 10^{-2}$  for  $\rho \geq 6$ .

### 3. Spinning bodies.

Most celestial bodies have spin; therefore it is interesting to study how intrinsic rotation would affect the evolution of the Kerr parameter for coalescing binaries.

As in the previous case, we shall confine ourselves to post-Newtonian corrections of order  $\gamma^2$  at most. Since spin-orbit and spin-spin interaction terms will affect the total mass only at order equal to or higher than  $\gamma^{5/2}$ , inclusion of spin will not change the equation (1) for the total mass. On the other hand, the post-Newtonian corrections to the angular momentum will include spin effects already at relative order  $\gamma^{3/2}$ . With the assumption of a slow precession of the orbital angular momentum and spins around the total angular

momentum, which is valid as long as  $\gamma \ll 1$  (Kidder 1995), we may take the equation for  $\mathbf{J}$  averaged over one orbit (Kidder 1995) and rewrite it with our notations as

$$\begin{aligned} \mathbf{J} = & \mu(Gmr)^{1/2}\hat{\mathbf{L}}_N \left(1 + 2\gamma - \left[(\hat{\mathbf{L}}_N \cdot \boldsymbol{\sigma}_1) \left(2 + \frac{7m_2}{4m_1}\right) + (\hat{\mathbf{L}}_N \cdot \boldsymbol{\sigma}_2) \left(2 + \frac{7m_1}{4m_2}\right)\right] \gamma^{3/2} + \right. \\ & \left. + \left\{ \frac{1}{2}(5 - 9\eta) - \frac{3}{4\eta}[(\boldsymbol{\sigma}_1 \cdot \boldsymbol{\sigma}_2) - 3(\hat{\mathbf{L}}_N \cdot \boldsymbol{\sigma}_1)(\hat{\mathbf{L}}_N \cdot \boldsymbol{\sigma}_2)] \right\} \gamma^2 + O(\gamma^{5/2}) \right) + \\ & + \mathbf{S}_1 \left[1 - \frac{1}{4}(3\eta + X_2)\gamma + O(\gamma^2)\right] + \mathbf{S}_2 \left[1 - \frac{1}{4}(3\eta + X_1)\gamma + O(\gamma^2)\right]. \end{aligned} \quad (3)$$

We now calculate the square power of  $J/M^2$  from equations (3) and (1) and obtain

$$\left(\frac{c}{G} \frac{J}{M^2}\right)^2 = \rho \left[A_0 + A_1\gamma^{1/2} + A_2\gamma + A_3\gamma^{3/2} + A_4\gamma^2 + O(\gamma^{5/2})\right], \quad (4)$$

where:

$$\left\{ \begin{array}{l} A_0 = \eta^2, \\ A_1 = 2\eta[\hat{\mathbf{L}}_N \cdot (\boldsymbol{\sigma}_1 + \boldsymbol{\sigma}_2)], \\ A_2 = 2\eta^2(2 + \eta) + \sigma_1^2 + \sigma_2^2 + 2(\boldsymbol{\sigma}_1 \cdot \boldsymbol{\sigma}_2), \\ A_3 = 2\eta[(\hat{\mathbf{L}}_N \cdot \boldsymbol{\sigma}_1)(2X_1 + \eta) + (\hat{\mathbf{L}}_N \cdot \boldsymbol{\sigma}_2)(2X_2 + \eta)], \\ A_4 = \frac{3}{2}\eta^2(6 - 3\eta + 2\eta^2) - \frac{1}{2}(1 + \eta)(\boldsymbol{\sigma}_1 \cdot \boldsymbol{\sigma}_2) - \frac{7}{2}(1 - \eta)(\hat{\mathbf{L}}_N \cdot \boldsymbol{\sigma}_1)(\hat{\mathbf{L}}_N \cdot \boldsymbol{\sigma}_2) + \\ \quad - \frac{X_2}{2}[X_2\sigma_1^2 + (\hat{\mathbf{L}}_N \cdot \boldsymbol{\sigma}_1)^2(8 - X_2)] - \frac{X_1}{2}[X_1\sigma_2^2 + (\hat{\mathbf{L}}_N \cdot \boldsymbol{\sigma}_2)^2(8 - X_1)]. \end{array} \right. \quad (5)$$

We shall deal with equation (4) rather than try to deduce a post-Newtonian expression for  $J/M^2$  as a truncated series because deciding which term in equation (4) is the leading one depends on the choice of the parameters  $\eta$ ,  $\chi_1$  and  $\chi_2$  and on the relative orientations of  $\hat{\mathbf{L}}_N$ ,  $\boldsymbol{\sigma}_1$  and  $\boldsymbol{\sigma}_2$ . As a matter of fact, if we focus on the first few terms of equation (4), we can write

$$\left(\frac{c}{G} \frac{J}{M^2}\right)^2 = [\eta\rho^{1/2}(1 + 2\gamma)\hat{\mathbf{L}}_N + \boldsymbol{\sigma}_1 + \boldsymbol{\sigma}_2]^2 + 2\eta^3 + O(\gamma^{1/2})$$

and notice that the Kerr parameter for spinning bodies depends mainly on the variables of the vector  $\eta\rho^{1/2}(1 + 2\gamma)\hat{\mathbf{L}}_N + \boldsymbol{\sigma}_1 + \boldsymbol{\sigma}_2$  (that is, the first post-Newtonian form of  $\mathbf{J}$  in units of  $Gm^2/c$ ) which determine the relative weight of the leading terms in equation (4). For example, if  $\chi_1 = \chi_2 = 1$  and  $\eta = \frac{1}{7}$  (which corresponds to a more massive body about 5 times as large as the other),  $A_2\gamma$  is of the same order of magnitude as  $A_0$  already at values of  $\rho \approx 50$  and greater at shorter separations. Let us remark that this does not imply that the second post-Newtonian formula (eq. [4]) is no longer valid at  $\rho \approx 50$ , because the

parameter of development of the post-Newtonian series is  $\gamma$  which does not depend on  $\eta$ ,  $\sigma_1$  and  $\sigma_2$ . We just point out that calculating  $J/M^2$  needs care.

As for the accuracy of equation (4), considerations quite similar to those stated in §2.1 about the post-Newtonian series (eq. [2]) apply. A thorough discussion should take into account the complicated form of the coefficients of the post-Newtonian series (eq. [4]; see eq. [5] and the unknown similar expressions for the neglected terms). Anyway, since such coefficients cannot be much larger than unity, the conclusions we reach are substantially equivalent.

As expected and already noticed, equation (4) depends on the relative orientations of the orbital and intrinsic angular momenta of the coalescing bodies, namely, on the quantities  $\hat{\mathbf{L}}_N \cdot \boldsymbol{\sigma}_1$ ,  $\hat{\mathbf{L}}_N \cdot \boldsymbol{\sigma}_2$ , and  $\boldsymbol{\sigma}_1 \cdot \boldsymbol{\sigma}_2$ , which are functions of the coordinate time  $t$  through  $r$ . Such functions were considered already by Cutler & Flanagan (1994) because of their importance to the secular growth of the gravitational wave phase. We performed a detailed analysis of these functions, finding results that we shall report in Appendix, since they have more general application than just in our problem. A related and interesting topic is also the evolution of the absolute orientations of  $\hat{\mathbf{L}}_N$ ,  $\boldsymbol{\sigma}_1$ ,  $\boldsymbol{\sigma}_2$ , since the observed gravitational waveform depends on the angle between the orbital plane—almost orthogonal to  $\hat{\mathbf{L}}_N$  with post-Newtonian corrections along  $\boldsymbol{\sigma}_1$  and  $\boldsymbol{\sigma}_2$ —and the wave propagation direction. This question is already fully examined in literature (Kidder 1995; Apostolatos et al. 1994), therefore we shall not consider it.

### 3.1. Effects of spin precession.

Here we shall deduce the equations to solve for determining the coefficients of equation (5) under the following two assumptions: first, that the spins precess while keeping constant absolute values and that the gravitational radiation emission only affects the orbital angular momentum  $\mathbf{L}$  (Apostolatos et al. 1994; Kidder 1995); second, that the precession frequency is much less than the orbital frequency. As analyzed by Kidder (1995) the ratio of the precession frequency to the orbital frequency goes as  $\gamma$ .

We are interested in the dependence on  $r$  of the scalar products between any pair of the three vectors  $\hat{\mathbf{L}}_N$ ,  $\boldsymbol{\sigma}_1$ ,  $\boldsymbol{\sigma}_2$ . We put together the equations for the orbital angular momentum, separation evolution, and spin precession (Kidder 1995) averaged over one orbit to lowest order and have

$$\mathbf{L}_N = \mu(Gmr)^{1/2}\hat{\mathbf{L}}_N, \quad \frac{dr}{dt} = -\frac{64}{5}c\eta\gamma^3,$$



$$\left\{ \begin{aligned} \frac{d\mathbf{L}_N}{dt} &= \frac{G}{2c^2r^3} \left\{ \left[ \left(4 + 3\frac{m_2}{m_1}\right) \mathbf{S}_1 + \left(4 + 3\frac{m_1}{m_2}\right) \mathbf{S}_2 \right] \times \mathbf{L}_N + \right. \\ &\quad \left. - 3[(\hat{\mathbf{L}}_N \cdot \mathbf{S}_2)\mathbf{S}_1 + (\hat{\mathbf{L}}_N \cdot \mathbf{S}_1)\mathbf{S}_2] \times \hat{\mathbf{L}}_N \right\} - \frac{32}{5} \frac{c^3}{G} \frac{\eta}{m} \gamma^4 \mathbf{L}_N, \\ \frac{d\mathbf{S}_1}{dt} &= \frac{G}{2c^2r^3} \left[ \left(4 + 3\frac{m_2}{m_1}\right) \mathbf{L}_N + \mathbf{S}_2 - 3(\hat{\mathbf{L}}_N \cdot \mathbf{S}_2)\hat{\mathbf{L}}_N \right] \times \mathbf{S}_1, \\ \frac{d\mathbf{S}_2}{dt} &= \frac{G}{2c^2r^3} \left[ \left(4 + 3\frac{m_1}{m_2}\right) \mathbf{L}_N + \mathbf{S}_1 - 3(\hat{\mathbf{L}}_N \cdot \mathbf{S}_1)\hat{\mathbf{L}}_N \right] \times \mathbf{S}_2. \end{aligned} \right. \quad (6)$$

Combining the above equations and rewriting the result in terms of dimensionless quantities we obtain:

$$\left\{ \begin{aligned} \frac{d}{d\rho}(\hat{\mathbf{L}}_N \cdot \boldsymbol{\sigma}_1) &= -\frac{15}{128\eta} \left[ \frac{1}{X_2} - \frac{(\hat{\mathbf{L}}_N \cdot \boldsymbol{\sigma}_1)}{\eta\rho^{1/2}} \right] (\hat{\mathbf{L}}_N \cdot \boldsymbol{\sigma}_1 \times \boldsymbol{\sigma}_2), \\ \frac{d}{d\rho}(\hat{\mathbf{L}}_N \cdot \boldsymbol{\sigma}_2) &= \frac{15}{128\eta} \left[ \frac{1}{X_1} - \frac{(\hat{\mathbf{L}}_N \cdot \boldsymbol{\sigma}_2)}{\eta\rho^{1/2}} \right] (\hat{\mathbf{L}}_N \cdot \boldsymbol{\sigma}_1 \times \boldsymbol{\sigma}_2), \\ \frac{d}{d\rho}(\boldsymbol{\sigma}_1 \cdot \boldsymbol{\sigma}_2) &= -\frac{15}{128\eta} \left[ \left( \frac{m_2}{m_1} - \frac{m_1}{m_2} \right) \eta\rho^{1/2} + (\hat{\mathbf{L}}_N \cdot \boldsymbol{\sigma}_1) + \right. \\ &\quad \left. - (\hat{\mathbf{L}}_N \cdot \boldsymbol{\sigma}_2) \right] (\hat{\mathbf{L}}_N \cdot \boldsymbol{\sigma}_1 \times \boldsymbol{\sigma}_2). \end{aligned} \right. \quad (7)$$

Expanding the quantity  $[\hat{\mathbf{L}}_N \times (\boldsymbol{\sigma}_1 \times \boldsymbol{\sigma}_2)]^2$  first according to the general rule for  $\mathbf{a} \times (\mathbf{b} \times \mathbf{c})$ , then according to that for  $(\mathbf{a} \times \mathbf{b}) \cdot (\mathbf{c} \times \mathbf{d})$ , we get an equation to close system (7):

$$\begin{aligned} (\hat{\mathbf{L}}_N \cdot \boldsymbol{\sigma}_1 \times \boldsymbol{\sigma}_2)^2 &= \sigma_1^2 \sigma_2^2 - (\boldsymbol{\sigma}_1 \cdot \boldsymbol{\sigma}_2)^2 - \sigma_1^2 (\hat{\mathbf{L}}_N \cdot \boldsymbol{\sigma}_2)^2 - \sigma_2^2 (\hat{\mathbf{L}}_N \cdot \boldsymbol{\sigma}_1)^2 + \\ &\quad + 2(\boldsymbol{\sigma}_1 \cdot \boldsymbol{\sigma}_2)(\hat{\mathbf{L}}_N \cdot \boldsymbol{\sigma}_1)(\hat{\mathbf{L}}_N \cdot \boldsymbol{\sigma}_2). \end{aligned} \quad (8)$$

The system of equations (7) contains nonlinear differential equations whose solutions have an oscillatory behavior. In order to avoid that a numerical integration stops when  $\hat{\mathbf{L}}_N \cdot \boldsymbol{\sigma}_1 \times \boldsymbol{\sigma}_2$  first reaches 0, we also differentiate equation (8) and substitute it with the

following:

$$\begin{aligned}
 \frac{d}{d\rho}(\hat{\mathbf{L}}_N \cdot \boldsymbol{\sigma}_1 \times \boldsymbol{\sigma}_2) &= -\frac{15}{128\eta} \left\{ (X_1 - X_2)[(\boldsymbol{\sigma}_1 \cdot \boldsymbol{\sigma}_2) - (\hat{\mathbf{L}}_N \cdot \boldsymbol{\sigma}_1)(\hat{\mathbf{L}}_N \cdot \boldsymbol{\sigma}_2)]\rho^{1/2} + \right. \\
 &\quad -(\hat{\mathbf{L}}_N \cdot \boldsymbol{\sigma}_1)(\boldsymbol{\sigma}_1 \cdot \boldsymbol{\sigma}_2)\frac{1 + X_1}{X_1} + (\hat{\mathbf{L}}_N \cdot \boldsymbol{\sigma}_2)(\boldsymbol{\sigma}_1 \cdot \boldsymbol{\sigma}_2)\frac{1 + X_2}{X_2} + \\
 &\quad +(\hat{\mathbf{L}}_N \cdot \boldsymbol{\sigma}_1)(\hat{\mathbf{L}}_N \cdot \boldsymbol{\sigma}_2)(\hat{\mathbf{L}}_N \cdot \boldsymbol{\sigma}_1 - \hat{\mathbf{L}}_N \cdot \boldsymbol{\sigma}_2) - \frac{\sigma_2^2}{X_2}(\hat{\mathbf{L}}_N \cdot \boldsymbol{\sigma}_1) + \\
 &\quad \left. + \frac{\sigma_1^2}{X_1}(\hat{\mathbf{L}}_N \cdot \boldsymbol{\sigma}_2) + \frac{\sigma_2^2(\hat{\mathbf{L}}_N \cdot \boldsymbol{\sigma}_1)^2 - \sigma_1^2(\hat{\mathbf{L}}_N \cdot \boldsymbol{\sigma}_2)^2}{\eta\rho^{1/2}} \right\}. \tag{9}
 \end{aligned}$$

We have solved the system of equations (7), (9) numerically for a few choices of the parameters  $\chi_1$ ,  $\chi_2$ ,  $X_1/X_2$  and of the initial values. Typical behaviors of the solutions to the above equations will be shown in the figures that illustrate the Appendix. We have judged the analysis of the system of equations (7), (9) explained in Appendix important for understanding the role of spin precession during coalescence, since in general the behavior of the relative orientations among  $\hat{\mathbf{L}}_N$ ,  $\boldsymbol{\sigma}_1$ , and  $\boldsymbol{\sigma}_2$  is not simply predictable: for example even the average values of the oscillating functions do not keep fixed but evolve, as can be seen in Figure 2—an example in which this effect is dramatic.

### 3.2. Results.

Once the evolution of  $\hat{\mathbf{L}}_N \cdot \boldsymbol{\sigma}_1$ ,  $\hat{\mathbf{L}}_N \cdot \boldsymbol{\sigma}_2$ ,  $\boldsymbol{\sigma}_1 \cdot \boldsymbol{\sigma}_2$  is known, we can deduce the behavior of the Kerr parameter from equations (4) and (5). Plots of this quantity for  $\chi_1 = \chi_2 = 1$  and different mass ratios are shown in Figure 3 (*solid lines*) and compared to the corresponding spinless case (*dashed lines*).

If the intrinsic spins of the bodies are not very small and if they are directed with a positive component along the orbital angular momentum, then the value of  $J/M^2$  remains larger than  $1(G/c)$  over the entire inspiral phase (Fig. 3a). When one body is much more massive than the other and its spin is initially positively oriented with the orbital angular momentum, then it contributes to keep the Kerr parameter larger than 1 even if the companion’s spin is negatively oriented, as shown in Fig. 3b. When both spins are negatively oriented with respect to the orbital angular momentum, then the Kerr parameter is less than in the corresponding spinless case, at least initially. In fact, at the end of the inspiral, the orbital angular momentum has been almost completely radiated away and only

the spin is left over, giving a positive contribution to  $J/M^2$  irrespective of its direction. For intermediate separations of the two bodies, it may happen that the spin corrections to  $J/M^2$  at different post-Newtonian orders add up to 0, as in the case of Figure 3c (notice the crossing of the two curves). It may also happen that total spin and orbital angular momentum have vanishing sum, as shown in Figure 3d (notice the solid curve approaching zero); if this phenomenon occurs before final coalescence, the evolution of the angular momenta is known as transitional precession (Apostolatos et al. 1994). In this last case the value of  $\rho$  at which  $J/M^2$  approaches zero varies with the system’s mass ratio and initial directions of the angular momenta. Thus there are particular choices of these values such that the Kerr parameter decreases almost to zero at the end of the inspiral phase; an example is shown in Figure 4 (the apparent flattening of the curve at  $\rho \approx 6$  is uncertain since the approximation there reaches its limit of validity). The need for special and uncommon choices (see discussion by Apostolatos et al. (1994), §IV.D.1) of the parameters in order to obtain a final vanishing total angular momentum makes us think that the formation of a Schwarzschild black hole, as result of coalescence of a compact binary, is a rare event.

The dynamics of inspiralling bodies and of their angular momenta, as described by the above formulae, is exactly the same even if the bodies are massive black holes. We can infer from our analysis that the end of the inspiral phase of coalescence of two black holes in the center of an active galactic nucleus is most likely characterized by conditions which are compatible with the formation of a fast rotating black hole.

Since  $J/M^2$  has a complicated dependence on  $\hat{\mathbf{L}}_N \cdot \hat{\mathbf{s}}_1$ ,  $\hat{\mathbf{L}}_N \cdot \hat{\mathbf{s}}_2$ ,  $\hat{\mathbf{s}}_1 \cdot \hat{\mathbf{s}}_2$ , and the parameters  $\eta$ ,  $\chi_1$ ,  $\chi_2$ , we computed the probability density function of  $cJ/(GM^2)$  at  $\rho = 6$  numerically (by the Monte Carlo method) for some plausible choices of parameters corresponding to neutron star binary systems. The probabilities of  $m_1$  and  $m_2$  were assumed uniformly distributed over an interval ranging from 1.2 to 1.6 (the scale does not matter) and the orientations of  $\hat{\mathbf{L}}_N$ ,  $\hat{\mathbf{s}}_1$ ,  $\hat{\mathbf{s}}_2$  were taken at random, with uniform probability, among all directions of space. The parameters  $\chi_1$  and  $\chi_2$  were also taken at random but with a probability distribution uniform in  $\log \chi$  and ranging from  $7.96 \times 10^{-5}$  (corresponding to the period of PSR J1951+1123, that is the largest known pulsar period; Camilo & Nice 1995) to 0.7 (corresponding to about the highest value compatible with rotational stability). The result is the extremely peaked function plotted in Figure 5a. It has a mean equal to 0.86 with standard deviation  $2.94 \times 10^{-2}$ , coefficient of skewness +7.67 and coefficient of excess (kurtosis) equal to +6.93. A normal distribution with same mean and deviation is plotted (without tails) for comparison (*dashed line*).

In Figure 5b the same distribution curve as in Figure 5a is compared to the probability distribution of  $J/M^2$  in the spinless case (again numerically calculated by the Monte Carlo

method and with the same assumed mass distribution function as before). This latter curve, dashed in figure, is even more peaked than the former, and it reaches its maximum at the value that equation (2) takes on for  $\rho = 6$  and  $\eta = \frac{1}{4}$ , that is  $J/M^2 \approx 0.8675(G/c)$ .

#### 4. Conclusions.

Neglecting finite size effects we examine the evolution of the Kerr parameter all the way up to the state in which the separation between the bodies is  $6Gm/c^2$  corresponding about to the onset of the dynamical instability of circular orbits. We found cases (for example, those shown in Figs. 5a and 5b) in which it remains larger than 1 (another instance was also found in the numerical study by Wilson, Mathews, & Marronetti 1996). This implies that the formation of a stationary black hole is possible in those cases only if  $J/M^2$  is decreased efficiently in the final dynamical phases of coalescence. As a matter of fact we cannot infer anything on the nature of the coalesced body in such cases. An argument like the one in the discussion by Cook (1994), concluding for a final Kerr parameter less than 1 without going through the full solution of the evolution problem, simply is not valid: first, because it would reach the same conclusion irrespectively of the value of  $J/M^2$  at the beginning of the dynamical phase (eq. [16] in that paper always gives  $J/M^2 \leq 1$ ); second, because it is based on the “a priori” not justified assumption of having a Kerr black hole at the end of the coalescence, and this already by itself implies that  $J/M^2 \leq 1$ .

Similarly the formation of a stationary neutron star seems highly unlikely in the absence of a powerfully dissipative mechanism, since we found that in all cases except a few very special ones  $J/M^2$  is still greater than  $0.7(G/c)$  at the end of the inspiral phase. Anyway, when the final coalesced object is a black hole, our results give us confidence that it is rapidly rotating (Cook 1994).

In the course of studying our main object, we had to deal with the problem of precessing spins. We found analytical solutions to the precession equations which we reported since they have a wider application than just to our purpose: that is, to the calculation of the gravitational wave modulation due to spin precession, as fully explained by Cutler & Flanagan (1994).

This work was partially supported by the Italian Space Agency (ASI), the Ministero della Università e della Ricerca Scientifica e Tecnologica (MURST) of Italy and by the GNFM of the Italian Consiglio Nazionale delle Ricerche (CNR). We would also thank the scientific editor, B. Haisch, and the anonymous referee for suggestions and positive criticisms that led to improvements of our paper.

### A. Analytical solutions of the precession equations.

A better insight into the behavior of the solutions to the system of differential equations (7), (8) is ensured by an analytical study of them. Because of the complexity of the problem, we have been able to obtain only approximate solutions for some cases. We have judged this analytical study useful because it applies also to the calculation of the gravitational waveform (Cutler & Flanagan 1994).

#### A.1. Preliminary considerations.

By elimination of  $\hat{\mathbf{L}}_N \cdot \boldsymbol{\sigma}_1 \times \boldsymbol{\sigma}_2$  from equation (7) we find two relations that do not involve  $\hat{\mathbf{L}}_N \cdot \boldsymbol{\sigma}_1 \times \boldsymbol{\sigma}_2$ , namely,

$$\begin{cases} \rho^{-1/2} \frac{d}{d\rho} (\boldsymbol{\sigma}_1 \cdot \boldsymbol{\sigma}_2) + \eta \frac{d}{d\rho} [\hat{\mathbf{L}}_N \cdot (\boldsymbol{\sigma}_1 + \boldsymbol{\sigma}_2)] = 0, \\ \rho^{-1/2} \frac{d}{d\rho} [(\hat{\mathbf{L}}_N \cdot \boldsymbol{\sigma}_1)(\hat{\mathbf{L}}_N \cdot \boldsymbol{\sigma}_2)] = \frac{d}{d\rho} [X_2(\hat{\mathbf{L}}_N \cdot \boldsymbol{\sigma}_1) + X_1(\hat{\mathbf{L}}_N \cdot \boldsymbol{\sigma}_2)]. \end{cases} \quad (\text{A1})$$

Equations (A1) are of the form  $d\psi/d\rho + \rho^{-1/2}d\varphi/d\rho = 0$ , hence an integration by parts yields  $\psi + \rho^{-1/2}\varphi + \frac{1}{2} \int \rho^{-3/2}\varphi(\rho) d\rho = 0$ , and since  $\varphi$  is in all cases at most of the order of unity, then for  $\rho \gg 1$ , this last equation leads to “approximate” first integrals in the following form:

$$\psi = \text{constant} + O(\rho^{-1/2}).$$

In order to deal with quantities which have manifestly the same order of magnitude, we find it convenient to rewrite the system of equations (7)–(8) in terms of the variables  $f$ ,  $g$ ,  $h$ , and  $V$ :

$$\frac{df}{d\rho} = -\frac{15}{128} \left( \frac{\chi_2}{X_1} - \chi_1 \chi_2 f \rho^{-1/2} \right) V, \quad (\text{A2})$$

$$\frac{dg}{d\rho} = \frac{15}{128} \left( \frac{\chi_1}{X_2} - \chi_1 \chi_2 g \rho^{-1/2} \right) V, \quad (\text{A3})$$

$$\frac{dh}{d\rho} = -\frac{15}{128} \left[ \left( \frac{X_2}{X_1} - \frac{X_1}{X_2} \right) \rho^{1/2} + \chi_1 \frac{X_1}{X_2} f - \chi_2 \frac{X_2}{X_1} g \right] V, \quad (\text{A4})$$

$$V^2 = 1 - f^2 - g^2 - h^2 + 2fgh. \quad (\text{A5})$$

Let us denote the initial values of  $f$ ,  $g$ ,  $h$ , and  $\rho$  by  $f_0$ ,  $g_0$ ,  $h_0$ , and  $\rho_0$  respectively, and the initial value of  $\hat{\mathbf{L}}_N \cdot \hat{\mathbf{s}}_1 \times \hat{\mathbf{s}}_2$ , with its sign, by  $V_0$ . Moreover we shall denote the initial value of the right-hand side of equation (9) by  $\sigma_1 \sigma_2 V'_0$ .

### A.2. One spinning body.

In the very special case where  $S_1 = 0$  or  $S_2 = 0$  “exactly”, we have

$$\hat{\mathbf{L}}_N \cdot \hat{\mathbf{s}}_1 = \text{constant} \quad (\text{if } S_2 = 0) ,$$

trivially from equation (6).

### A.3. Equal masses.

Let  $X_1 = X_2$  and thus  $\eta = 1/4$ . Then the first term in the right-hand side of equation (A4) vanishes. Moreover from equations (A1) we obtain the following first integral “exactly” (in the sense that it is a necessary consequence of eq. [A1], with no need for any further approximation):

$$h + \frac{1}{2}fg = \text{constant}. \quad (\text{A6})$$

On the other hand, if  $\rho \gg 1$ , we can neglect the terms containing  $\rho^{-1/2}$  in the right-hand sides of equations (A2) and (A3) and take either equation in (A1) (but not both) to give an “approximate” first integral as (cf. eq. 46 in Apostolatos et al. 1994)

$$\chi_1 f + \chi_2 g = \text{constant}. \quad (\text{A7})$$

Summing up, we can approximate the system of equations (A2)–(A5) with the following autonomous differential system:

$$\left\{ \begin{array}{l} \frac{df}{d\rho} = -\frac{15}{64}\chi_2 V, \\ \frac{dg}{d\rho} = \frac{15}{64}\chi_1 V, \\ \frac{dh}{d\rho} = -\frac{15}{128}(\chi_1 f - \chi_2 g)V, \\ V^2 = 1 - f^2 - g^2 - h^2 + 2fgh, \end{array} \right. \quad (\text{A8})$$

whose integral lines in the  $(f, g, h)$ -space are arcs of parabolas given by the following

conditions

$$\begin{cases} h + \frac{1}{2}fg = \text{constant}, \\ \chi_1 f + \chi_2 g = \text{constant}, \\ 1 - f^2 - g^2 - h^2 + 2fgh \geq 0. \end{cases}$$

We can set a new parameter  $u$  as

$$u = \frac{\chi_2}{\sqrt{\chi_1^2 + \chi_2^2}}(f - f_0) - \frac{\chi_1}{\sqrt{\chi_1^2 + \chi_2^2}}(g - g_0)$$

and write  $f$  and  $g$  as follows

$$f = f_0 + \frac{\chi_2}{\sqrt{\chi_1^2 + \chi_2^2}}u, \quad g = g_0 - \frac{\chi_1}{\sqrt{\chi_1^2 + \chi_2^2}}u. \quad (\text{A9})$$

Substituting equations (A9) into equation (A6) and both equations (A6) and (A9) repeatedly into equation (A8), we can finally reduce the system of equations (A8) to quadrature:

$$\left\{ \begin{array}{l} h(u) = h_0 - \frac{(\chi_1 f_0 - \chi_2 g_0)^2}{8\chi_1 \chi_2} + \frac{\chi_1 \chi_2}{2(\chi_1^2 + \chi_2^2)} \left[ u - \frac{\sqrt{\chi_1^2 + \chi_2^2}}{2\chi_1 \chi_2} (\chi_2 g_0 - \chi_1 f_0) \right]^2, \\ V^2(u) = 1 - \frac{(\chi_1 f_0 + \chi_2 g_0)^2}{\chi_1^2 + \chi_2^2} + \frac{1}{5}(2h_0 + f_0 g_0)^2 + \\ \quad - \left[ u - \frac{(\chi_1 g_0 - \chi_2 f_0)}{\sqrt{\chi_1^2 + \chi_2^2}} \right]^2 - 5 \left[ h(u) - \frac{1}{5}(2h_0 + f_0 g_0) \right]^2, \\ \frac{du}{d\rho} = -\frac{15}{64} \sqrt{\chi_1^2 + \chi_2^2} V(u). \end{array} \right. \quad (\text{A10})$$

The solution,

$$-\frac{15}{64} \sqrt{\chi_1^2 + \chi_2^2} (\rho - \rho_0) = \int_0^u \frac{dv}{V(v)}, \quad (\text{A11})$$

involves an elliptic integral of the first kind, so that  $u$  can be expressed in terms of the Jacobian elliptic functions (Abramowitz & Stegun 1964, p. 596). Let us remark that the oscillation period is inversely proportional to  $(\chi_1^2 + \chi_2^2)^{1/2}$  and that the turning points of  $u$ , i.e., the zeros of  $V(u)$ , are given by the intersection in the  $(u, h)$ -plane of the parabola

$$h = h_0 - \frac{(\chi_1 f_0 - \chi_2 g_0)^2}{8\chi_1 \chi_2} + \frac{\chi_1 \chi_2}{2(\chi_1^2 + \chi_2^2)} \left[ u - \frac{\sqrt{\chi_1^2 + \chi_2^2}}{2\chi_1 \chi_2} (\chi_2 g_0 - \chi_1 f_0) \right]^2$$

with the ellipse

$$\begin{aligned} \left[ u - \frac{(\chi_1 g_0 - \chi_2 f_0)}{\sqrt{\chi_1^2 + \chi_2^2}} \right]^2 + 5 \left[ h - \frac{1}{5}(2h_0 + f_0 g_0) \right]^2 = \\ = 1 - \frac{(\chi_1 f_0 + \chi_2 g_0)^2}{\chi_1^2 + \chi_2^2} + \frac{1}{5}(2h_0 + f_0 g_0)^2. \end{aligned}$$

We can also notice that the oscillation amplitude depends on  $\chi_1$  and  $\chi_2$  only through their relative weight (e.g., the quantity  $\chi_1/\chi_2$  or its reciprocal) and is independent from their absolute magnitudes. In fact, the oscillation amplitude is determined only by the right-hand side of equation (A11), in which  $V(v)$  is a homogeneous function of  $\chi_1$  and  $\chi_2$  with degree zero, as an inspection of equation (A10) readily shows.

Let us finally observe that the approximation condition  $X_1 = X_2$  may in practice be replaced by the condition  $|X_1 - X_2|\rho^{1/2} \ll \min\{\chi_1, \chi_2\}$  sufficient for the first term in equation (A4) to be negligible.

### A.3.1. Examples.

1.  $\chi_1 = \chi_2 = \chi \neq 0$ . We have from equation (A10) :

$$\begin{cases} h = h_0 - \frac{1}{4}u_*^2 + \frac{1}{4}(u - u_*)^2, \\ V^2 = \frac{5}{16} \left[ \frac{8}{5}(\sqrt{\Delta} + a - \frac{5}{8}u_*^2) + (u - u_*)^2 \right] \left[ \frac{8}{5}(\sqrt{\Delta} - a + \frac{5}{8}u_*^2) - (u - u_*)^2 \right], \end{cases} \quad (\text{A12})$$

where  $u_* = (g_0 - f_0)/2^{1/2}$ ,  $a = 1 + (3h_0 - f_0 g_0)/2$ ,  $\Delta = a^2 + 5V_0^2/4$ . Equation (A11) can be integrated now by direct application of one of the formulae on p. 596 of (Abramowitz & Stegun 1964), the selection of which depends on the signs of the quantities  $a - 5u_*^2/8 \pm \Delta^{1/2}$ . For example, if we suppose that  $u_* = 0$ , that is  $f_0 = g_0$ , then  $a + \Delta^{1/2} \geq 0$  and  $a - \Delta^{1/2} \leq 0$ . The solution is then

$$u(\rho) = -\text{sign}(V_0) \sqrt{\frac{4(\Delta - a^2)}{5\sqrt{\Delta}}} \text{sd} \left( \frac{15}{64} \chi^4 \sqrt{4\Delta} (\rho - \rho_0) \middle| \frac{\sqrt{\Delta} - a}{2\sqrt{\Delta}} \right), \quad (\text{A13})$$

where “sd” is the well-known Jacobian elliptic function, equivalent to the function “cn” modulo a translation and a rescaling:  $\text{sd}(v|y) = \text{cn}(v - K(y)|y)/(1 - y)^{1/2}$  [see eq. (16.8.2) in Abramowitz & Stegun 1964; from now on  $K(y)$  is the complete elliptic integral of the first kind with parameter  $y$ , as defined by eq. (17.3.1) in the last reference]. As  $\rho$  varies,  $u(\rho)$  oscillates with a period

$$\lambda = \frac{256 K\left(\frac{\sqrt{\Delta} - a}{2\sqrt{\Delta}}\right)}{15^4 \sqrt{4\Delta} \chi}. \quad (\text{A14})$$



The analytic equations (A12), (A13), and (A14) show the dependence on the initial conditions  $f_0$ ,  $g_0$ ,  $h_0$  explicitly. Let us notice that the amplitude of oscillations does not depend on  $\chi$ , in this case. A plot of  $f(\rho)$  and  $V(\rho)$ , together with the numerical solution of equations (A2)–(A5) for comparison, is shown in Figure 6 for the choice of  $\rho_0 = 75$ ,  $f_0 = g_0 = 0.25$ ,  $h_0 = -0.5$ ,  $V_0 = -0.75$ ,  $\chi_1 = 1$ ,  $\chi_2 = 1$ , corresponding to Figure 12 of (Abramovici et al. 1992). Here we have  $a = 7/32 \approx 0.22$ ,  $\Delta = 769/1024 \approx 0.75$ . In this case we notice that, close to the last stable orbit, the agreement between analytical and numerical calculations becomes slightly less satisfactory.

2.  $\chi_1/\chi_2 \rightarrow 0$ . We have from equations (A9) and (A6) that  $f = f_0 + u$ ,  $g = g_0$  and  $h = h_0 - g_0 u/2$ . Thus, equation (A5) yields

$$V^2(u) = a^2 - b^2(u - u_*)^2,$$

where  $b^2 = 1 + 5g_0^2/4$ ,  $u_* = (3g_0h_0 - 2f_0 - f_0g_0^2)/(2b^2)$ ,  $a^2 = V_0^2 + b^2u_*^2$ . Therefore the equation  $du/d\rho = -15\chi_2V(u)/64$  is easily integrated and yields

$$u(\rho) = u_* - (\text{sign}V_0)\frac{a}{b} \sin \left[ \frac{15}{64}b\chi_2(\rho - \rho_0) + (\text{sign}V_0)\varphi \right], \quad (\text{A15})$$

where  $\sin \varphi = bu_*/a$ . As  $\rho$  varies  $u$  oscillates with a period given by the following expression

$$\lambda = \frac{128\pi}{15\sqrt{1 + 5g_0^2/4} \chi_2}, \quad (\text{A16})$$

in perfect agreement<sup>4</sup> with formula (B25) of (Cutler & Flanagan 1994).

3.  $f_0 = g_0 = 0$ . We have from equation (A10) that the following relations hold:

$$\begin{cases} h = h_0 + \frac{\Gamma}{2}u^2, \\ V^2 = \frac{5}{4}\Gamma^2(u^2 + a^2)(b^2 - u^2), \end{cases} \quad (\text{A17})$$

where we have defined the following constants:  $\Gamma = \chi_1\chi_2/(\chi_1^2 + \chi_2^2)$ ,  $a^2 = \{2[1 + 6h_0\Gamma + (5 + 4h_0^2)\Gamma^2]^{1/2} + 2 + 6h_0\Gamma\}/(5\Gamma^2)$  and  $b^2 =$

---

<sup>4</sup>There are a few minor typographic errors in Appendix B of (Cutler & Flanagan 1994). Equations (B14), (B20) and (B25) should read  $h_4 = -15(s_2\alpha_{2,i} + L\delta)/(128\mu)$ ,  $\kappa^2 = 1 - \alpha_{2,i}^2 - (1 - \alpha_{2,i}^2)\alpha_{-,i}^2/\nu_0^2$  and  $\nu_0^2 = [225/4096 + 1125\alpha_{2,i}^2/16384] s_2^2/\mu^2$  respectively.

$\{2[1 + 6h_0\Gamma + (5 + 4h_0^2)\Gamma^2]^{1/2} - 2 - 6h_0\Gamma\}/(5\Gamma^2)$ . The solution is

$$u(\rho) = \frac{-\text{sign}(V_0)ab}{\sqrt{a^2 + b^2}} \text{sd} \left( \frac{15}{128} \sqrt{5(\chi_1^2 + \chi_2^2)\Gamma^2(a^2 + b^2)}(\rho - \rho_0) \left| \frac{b^2}{a^2 + b^2} \right. \right). \quad (\text{A18})$$

As  $\rho$  varies  $u$  oscillates with a period

$$\lambda = \frac{256 K(b^2/(a^2 + b^2))}{15\sqrt{\chi_1^2 + \chi_2^2} \sqrt[4]{1 + 6h_0\Gamma + (5 + 4h_0^2)\Gamma^2}}. \quad (\text{A19})$$

The analytic equations (A17), (A18), and (A19) show the dependence on  $\chi_1$  and  $\chi_2$  explicitly. Both the oscillation amplitude and period depend on  $\chi_1$  and  $\chi_2$  in this case, but the amplitude depends only on  $\Gamma$  and not on  $(\chi_1^2 + \chi_2^2)^{1/2}$ , as previously noticed. Let us remark that in the limit  $\chi_1 \ll \chi_2$  we find for equations (A18) and (A19) the same expressions given in the example (2) by equations (A15) and (A16) with  $f_0 = g_0 = 0$ , as is easily seen when we notice that, if  $\chi_1 \ll \chi_2$ , then  $\Gamma \sim \chi_1/\chi_2$ ,  $a^2 \sim 4\chi_2^2/(5\chi_1^2)$ ,  $b^2 \sim 1 - h_0^2$ , and that  $\lim_{y \rightarrow 0} \text{sd}(v|y) = \sin v$ .

We plot in Figure 7 the analytical solutions (*solid line*) and the numerical solutions (*dots*) for  $f(\rho)$  and  $V(\rho)$ , with the chosen values  $\chi_1 = 10^{-3}$ ,  $\chi_2 = 1$ ,  $f_0 = g_0 = h_0 = 0$  and  $\rho_0 = 250$ . As we see, the agreement between the analytical and the numerical curves is striking.

#### A.4. Very different masses at large separations.

By differentiating equation (A5) twice with respect to  $\rho$  and making repeated use of equations (A2)–(A4), we obtain  $d^2V/d\rho^2 = F(f, g, h, \rho)$  where  $F$  is an algebraic function, easily calculated. If  $|X_1 - X_2|\rho^{1/2} \gg 1$ , then the leading term in  $F$  is much greater than all others and the equation for  $V$  is approximated by the following one

$$\frac{d^2V}{d\rho^2} = - \left( \frac{15}{128} \frac{X_1 - X_2}{\eta} \right)^2 \rho V(\rho),$$

whose solution is

$$V(\rho) = C_1 \text{Ai}(-\Omega^{2/3}\rho) + C_2 \text{Bi}(-\Omega^{2/3}\rho), \quad (\text{A20})$$

where Ai and Bi are the Airy functions (fully described in Appendix b of Landau & Lifshitz 1958 and §10.4 of Abramowitz & Stegun 1964),  $\Omega = 15|X_1 - X_2|/(128\eta)$ ,  $C_1$  and  $C_2$  are

integration constants such that  $V(\rho_0) = V_0$  and  $[dV/d\rho]_{\rho_0} = V'_0$ , namely,

$$\begin{cases} C_1 = \frac{V_0 \text{Bi}'(-\Omega^{2/3}\rho_0) + V'_0 \Omega^{-2/3} \text{Bi}(-\Omega^{2/3}\rho_0)}{\text{Ai}(-\Omega^{2/3}\rho_0) \text{Bi}'(-\Omega^{2/3}\rho_0) - \text{Ai}'(-\Omega^{2/3}\rho_0) \text{Bi}(-\Omega^{2/3}\rho_0)}, \\ C_2 = \frac{V_0 \text{Ai}'(-\Omega^{2/3}\rho_0) + V'_0 \Omega^{-2/3} \text{Ai}(-\Omega^{2/3}\rho_0)}{\text{Ai}'(-\Omega^{2/3}\rho_0) \text{Bi}(-\Omega^{2/3}\rho_0) - \text{Ai}(-\Omega^{2/3}\rho_0) \text{Bi}'(-\Omega^{2/3}\rho_0)}. \end{cases}$$

We then get, by truncating equations (A2)–(A4) to the lowest order terms in  $\rho$ , the following approximate solutions:

$$\begin{cases} f(\rho) = f_0 - \frac{15}{128} \frac{\chi_2}{X_1} \int_{\rho_0}^{\rho} V(y) dy, \\ g(\rho) = g_0 + \frac{15}{128} \frac{\chi_1}{X_2} \int_{\rho_0}^{\rho} V(y) dy, \\ h(\rho) = h_0 + \frac{15}{128} \frac{X_1 - X_2}{\eta} \int_{\rho_0}^{\rho} y^{1/2} V(y) dy, \end{cases} \quad (\text{A21})$$

where  $V(\rho)$  is given by equation (A20).

For the evaluation of equations (A21) we need to know the functions  $\int^y \text{Ai}(-y) dy$  and  $\int^y \text{Bi}(-y) dy$ , which are tabulated in Table 10.12 of (Abramowitz & Stegun 1964), or asymptotic expansions for them (valid if both  $\rho$  and  $\rho_0$  are much greater than unity), which we adapted from equations (10.4.83) and (10.4.85) of (Abramowitz & Stegun 1964) and give here for reference:

$$\begin{cases} \int_{\rho_0}^{\rho} \text{Ai}(-\Omega^{2/3}y) dy \sim -\pi^{-1/2} \Omega^{-7/6} \left[ y^{-3/4} \cos\left(\frac{2}{3}\Omega y^{3/2} + \frac{\pi}{4}\right) \right]_{\rho_0}^{\rho}, \\ \int_{\rho_0}^{\rho} \text{Bi}(-\Omega^{2/3}y) dy \sim +\pi^{-1/2} \Omega^{-7/6} \left[ y^{-3/4} \sin\left(\frac{2}{3}\Omega y^{3/2} + \frac{\pi}{4}\right) \right]_{\rho_0}^{\rho}. \end{cases}$$

We also need the following formulae, which we worked out with the help of equations (10.4.60) and (10.4.64) in (Abramowitz & Stegun 1964):

$$\begin{cases} \int_{\rho_0}^{\rho} y^{1/2} \text{Ai}(-\Omega^{2/3}y) dy \sim -\pi^{-1/2} \Omega^{-7/6} \left[ y^{-1/4} \cos\left(\frac{2}{3}\Omega y^{3/2} + \frac{\pi}{4}\right) \right]_{\rho_0}^{\rho}, \\ \int_{\rho_0}^{\rho} y^{1/2} \text{Bi}(-\Omega^{2/3}y) dy \sim +\pi^{-1/2} \Omega^{-7/6} \left[ y^{-1/4} \sin\left(\frac{2}{3}\Omega y^{3/2} + \frac{\pi}{4}\right) \right]_{\rho_0}^{\rho}. \end{cases}$$

If  $X_1 \neq X_2$ , the condition  $|X_1 - X_2|\rho^{1/2} \gg 1$  for the validity of the approximation can always apply at sufficiently large values of  $\rho$ , but the agreement becomes increasingly

poorer as  $\rho$  decreases. In fact, at short separations the solution given by equations (A21) fails to predict both the period and the amplitude of oscillations to a sufficient degree of accuracy. Nevertheless this solution is worth being considered because it is very simple and approximately describes the behavior of the system in a large variety of cases.

## REFERENCES

- Abramovici, A., et al. 1992, *Science*, 256, 325
- Abramowitz, M. & Stegun, I. A., eds. 1964, *Handbook of Mathematical Functions*, (Washington D.C.: U. S. National Bureau of Standards)
- Apostolatos, T. A., Cutler, C., Sussman, G. J., & Thorne, K. S. 1994, *Phys. Rev. D*, 49, 6274
- Batten, A. H. 1973, *Binary and Multiple Systems of Stars*, (Oxford: Pergamon Press)
- Blanchet, L. 1996, *Phys. Rev. D*, 54, 1417
- Blanchet, L., Damour, T., & Iyer, B. R. 1995, *Phys. Rev. D*, 51, 5360
- Camilo, F. & Nice, D. J. 1995, *ApJ*, 445, 756
- Cook, G. B. 1994, *Phys. Rev. D*, 50, 5025
- Cook, G. B., Shapiro, S. L. & Teukolsky, S. A. 1994, *ApJ*, 424, 823
- Cutler, C. & Flanagan, É. E. 1994, *Phys. Rev. D*, 49, 2658
- Damour, T. 1987, in *300 Years of Gravitation*, ed. S. Hawking & W. Israel (Cambridge: Cambridge Univ. Press), 128
- de Felice, F. & Yunqiang, Y. 1982, *J. Phys. A: Math. Gen.*, 15, 3341
- Friedman, J. L. & Ipser, J. R. 1992, *Philos. Trans. R. Soc. London*, A340, 391
- Junker, W. & Schäfer, G. 1992, *MNRAS*, 254, 146
- Kidder, L. E. 1995, *Phys. Rev. D*, 52, 821
- Kidder, L. E., Will, C. M. & Wiseman, A. G. 1993, *Phys. Rev. D*, 47, 3281
- Lai, D. & Wiseman, A. G. 1996, *Phys. Rev. D*, 54, 3958
- Landau, L. D. & Lifshitz, E. M. 1958, in *Course of Theoretical Physics, Vol. 3, Quantum Mechanics, Non-relativistic Theory*, (London: Pergamon Press), Appendix B
- Lincoln, C. W. & Will, C. M. 1990, *Phys. Rev. D*, 42, 1123
- Narayan, R. T., Piran, & Shemi, A. 1991, *ApJ*, 379, L17

- Peters, P. C. 1964, *Phys. Rev.*, 136, B1224
- Phinney, E. S. 1991, *ApJ*, 380, L17
- Poisson, E. 1995, *Phys. Rev. D*, 52, 5719
- Salgado, M., Bonazzola, S., Gourgoulhon, E. & Haensel, P. 1994, *A&A*, 291, 155
- Salgado, M., Bonazzola, S., Gourgoulhon, E. & Haensel, P. 1994, *A&ASuppl.*, 108, 455
- Schutz, B. F. 1986, *Nature*, 323, 310
- Schutz, B. F. 1996, *Class. Quantum Grav.*, 13, A219
- Simone, L. E., Leonard, S. W., Poisson, E. & Will, C. M. 1997, *Class. Quantum Grav.*, 14, 237
- Thorne, K. S. 1987, in *300 Years of Gravitation*, ed. S. Hawking & W. Israel (Cambridge: Cambridge Univ. Press), 330
- Tutukov, A. V. & Yungelson, L. R. 1993, *MNRAS*, 260, 675
- Wagoner, R. V. & Will, C. M. 1976, *ApJ*, 210, 764
- Will, C. M. & Wiseman, A. G. 1996, *Phys. Rev. D*, 54, 4813
- Wilson, J. R., Mathews, G. J., & Marronetti, P. 1996, *Phys. Rev. D*, 54, 1317
- Yamaoka, H., Shigeyama, T. & Nomoto, K. 1993, *A&A*, 267, 433

**Figure captions.**

Fig. 1. Contour lines  $cJ/(GM^2) = 0.25, 0.50, \dots, 2.50$  in the  $(\rho, \eta)$ -plane.

Fig. 2. Evolution of  $\hat{\mathbf{L}}_N \cdot \boldsymbol{\sigma}_1$  from  $\rho = 75$  to  $\rho = 6$  for a system with  $m_2 = 0.13m_1$  with the following choice of initial values:  $(\hat{\mathbf{L}}_N \cdot \boldsymbol{\sigma}_1)_0 = -0.78256$ ,  $(\hat{\mathbf{L}}_N \cdot \boldsymbol{\sigma}_2)_0 = -1.1177 \times 10^{-4}$ ,  $(\boldsymbol{\sigma}_1 \cdot \boldsymbol{\sigma}_2)_0 = -8.7585 \times 10^{-5}$ ,  $(\hat{\mathbf{L}}_N \cdot \boldsymbol{\sigma}_1 \times \boldsymbol{\sigma}_2)_0 = -3.6197 \times 10^{-4}$ .

Fig. 3. Behavior of the Kerr parameter as function of  $\rho$  when  $\chi_1 = \chi_2 = 1$  (*solid lines*) and

(a)  $m_1 = m_2$ ;  $f_0 = g_0 = 0.9$ ,  $h_0 = 0.63$  at  $\rho_0 = 100$ .

(b)  $m_2 = 0.1m_1$ ;  $f_0 = -g_0 = 0.9$ ,  $h_0 = -0.7$  at  $\rho_0 = 100$ .

(c)  $m_2 = 0.1m_1$ ;  $f_0 = -0.42555$ ,  $g_0 = -0.59746$ ,  $h_0 = 0.23651$  at  $\rho_0 = 180$ .

(d)  $m_2 = 0.13m_1$ ;  $f_0 = -0.999247282$ ,  $g_0 = -8.44485 \times 10^{-3}$ ,  $h_0 = -8.45 \times 10^{-3}$  at  $\rho_0 = 75$ , which is the same choice as for Fig. 2.

The corresponding spinless cases are shown for comparison (*dashed lines*).

Fig. 4. Decrease of the Kerr parameter almost to zero at the end of the inspiral phase is obtained only for particular choices of parameters and initial conditions. In this case we have  $m_2 = 10m_1$ ,  $\chi_1 = \chi_2 = 0.351$  and  $f_0 = -g_0 = -h_0 = 1$  at  $\rho_0 = 100$ .

Fig. 5. (a) Probability density function of  $cJ/(GM^2)$  at  $\rho = 6$  computed by the Monte Carlo method. Assumptions for the probability distributions of parameters and relative orientations of angular momenta are explained in text. A normal distribution with same mean and standard deviation is plotted for comparison. (b) Comparison of the same curve as in (a) with the probability density function of  $cJ/(GM^2)$  at  $\rho = 6$  for the spinless case (*dashed line*), numerically computed. Notice that the figure scale is different from (a) to (b).

Fig. 6. Plots of (a)  $f = \hat{\mathbf{L}}_N \cdot \hat{\mathbf{s}}_1$ , (b)  $V = \hat{\mathbf{L}}_N \cdot \hat{\mathbf{s}}_1 \times \hat{\mathbf{s}}_2$  versus separation  $\rho$ , when  $\rho_0 = 75$ ;  $f_0 = g_0 = 0.25$ ,  $h_0 = -0.5$ ,  $V_0 = -0.75$ ;  $\chi_1 = \chi_2 = 1$  and  $m_1 = m_2$ . Solid lines show the analytical solutions, dots show the numerical solutions to equations (A2)–(A5).

Fig. 7. Plots of (a)  $f = \hat{\mathbf{L}}_N \cdot \hat{\mathbf{s}}_1$ , (b)  $V = \hat{\mathbf{L}}_N \cdot \hat{\mathbf{s}}_1 \times \hat{\mathbf{s}}_2$  versus separation  $\rho$ , when  $\rho_0 = 250$ ;  $f_0 = g_0 = h_0 = 0$ ;  $V_0 = -1$ ;  $\chi_1 = 10^{-3}$ ,  $\chi_2 = 1$  and  $m_1 = m_2$ . Solid lines show the analytical solutions, dots show the numerical solutions to equations (A2)–(A5).

# Figure 1

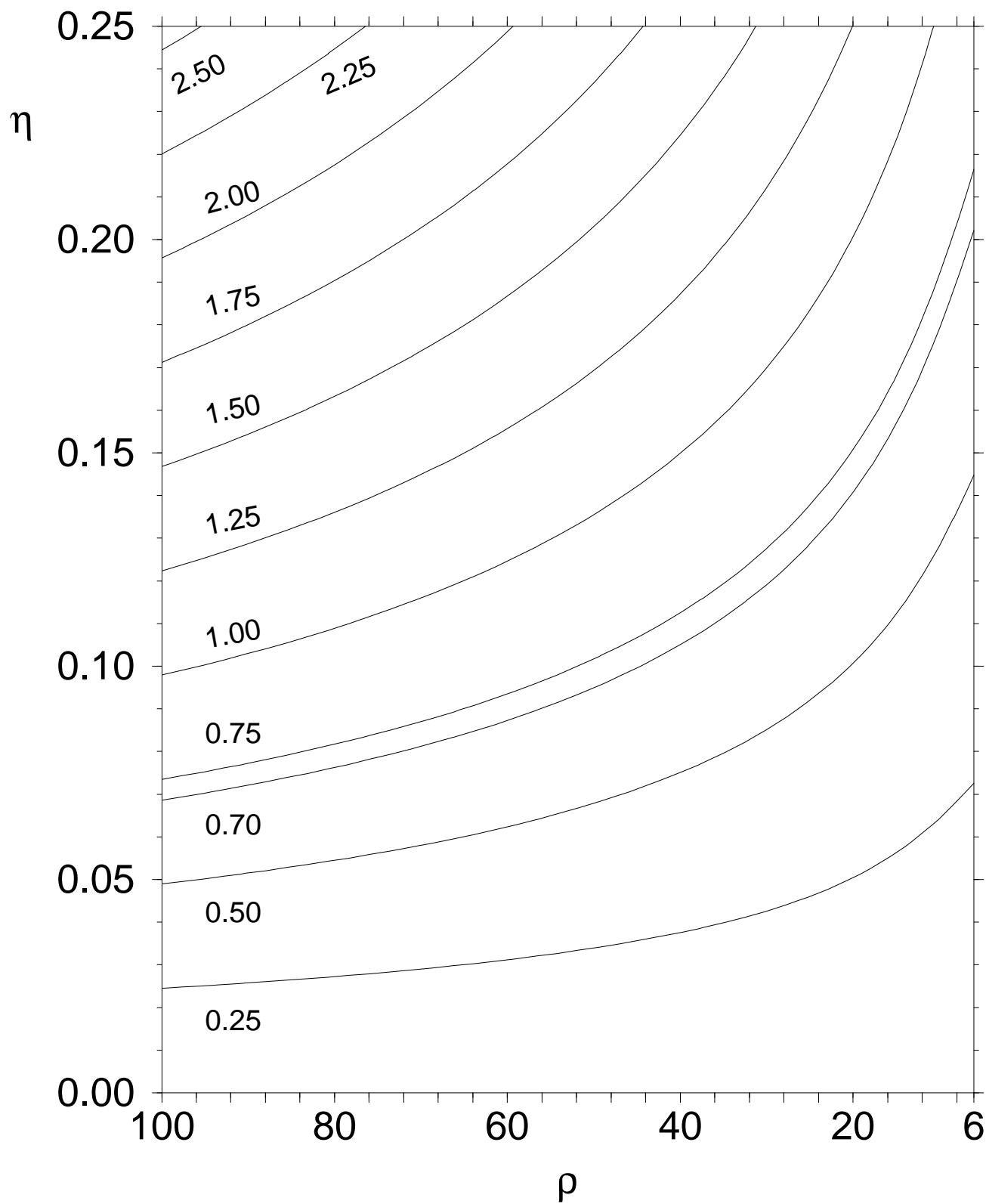




Figure 2

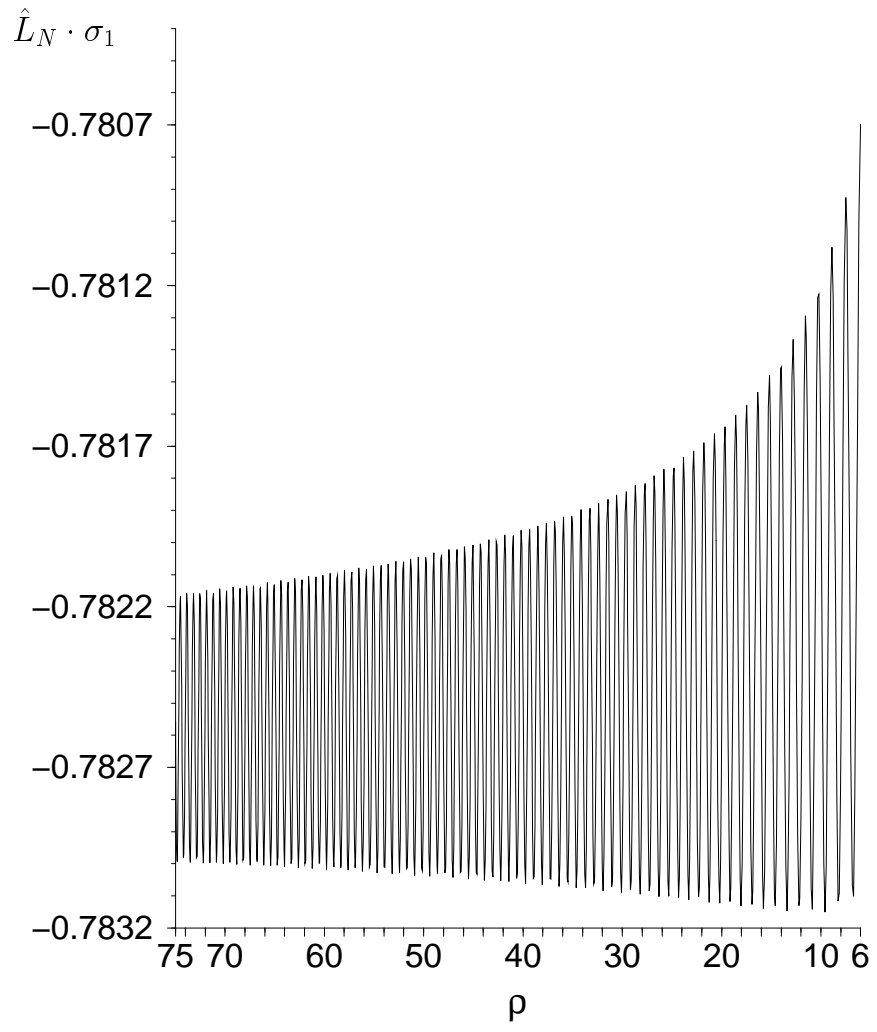


Figure 3a

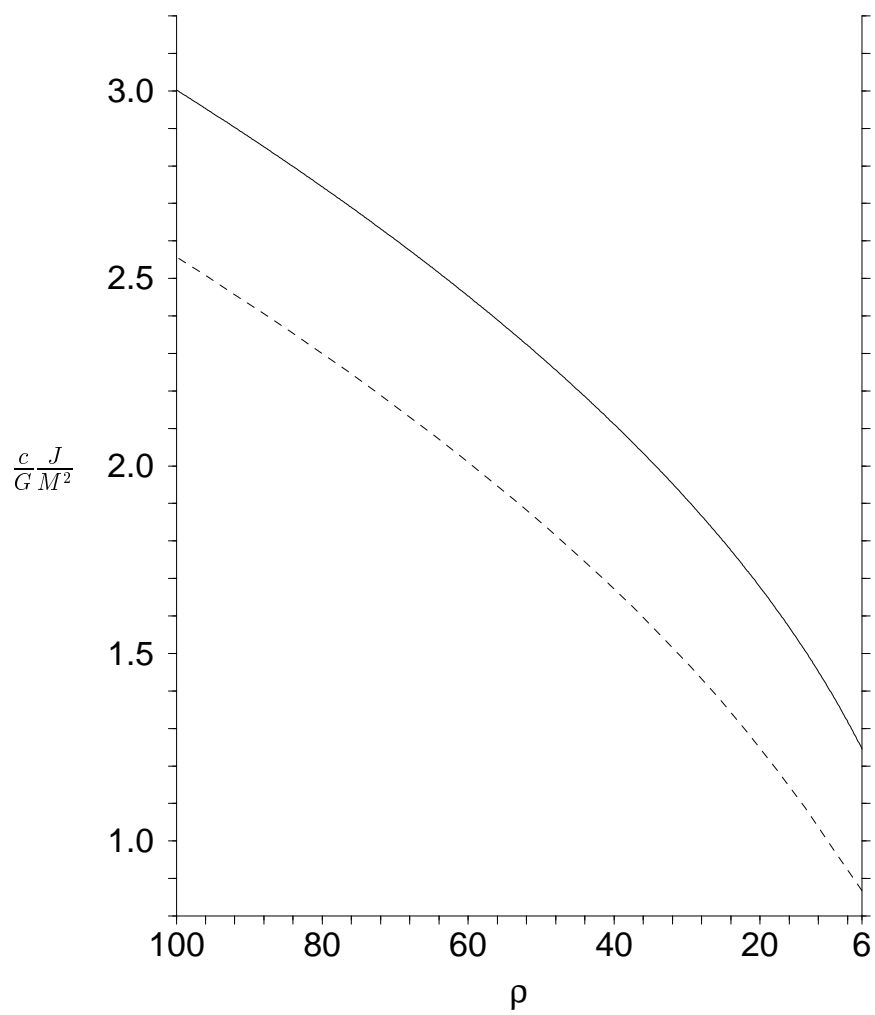


Figure 3b

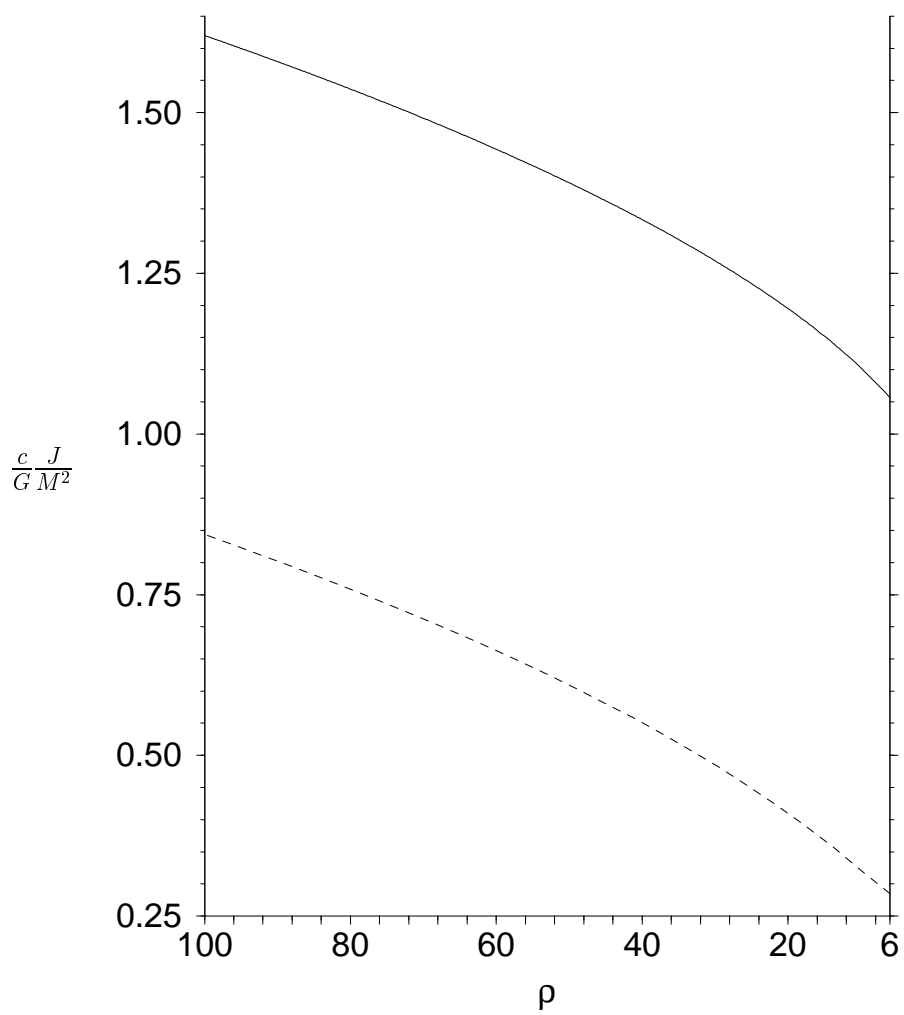


Figure 3c

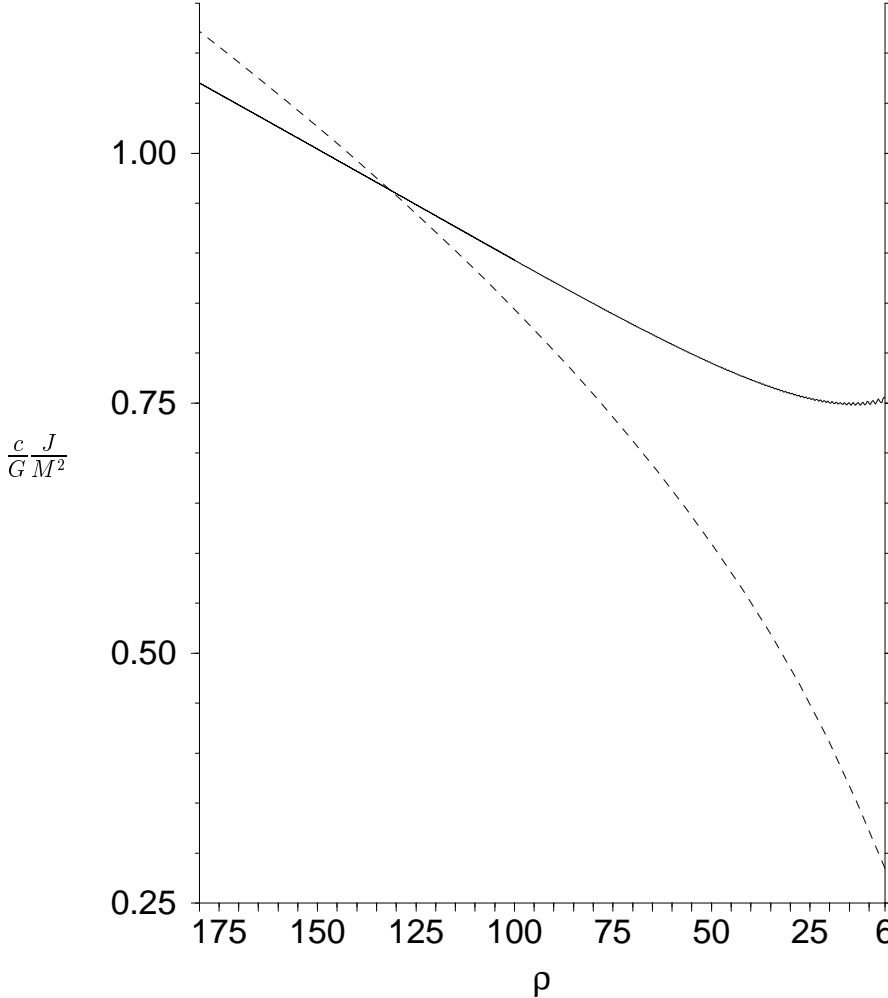


Figure 3d

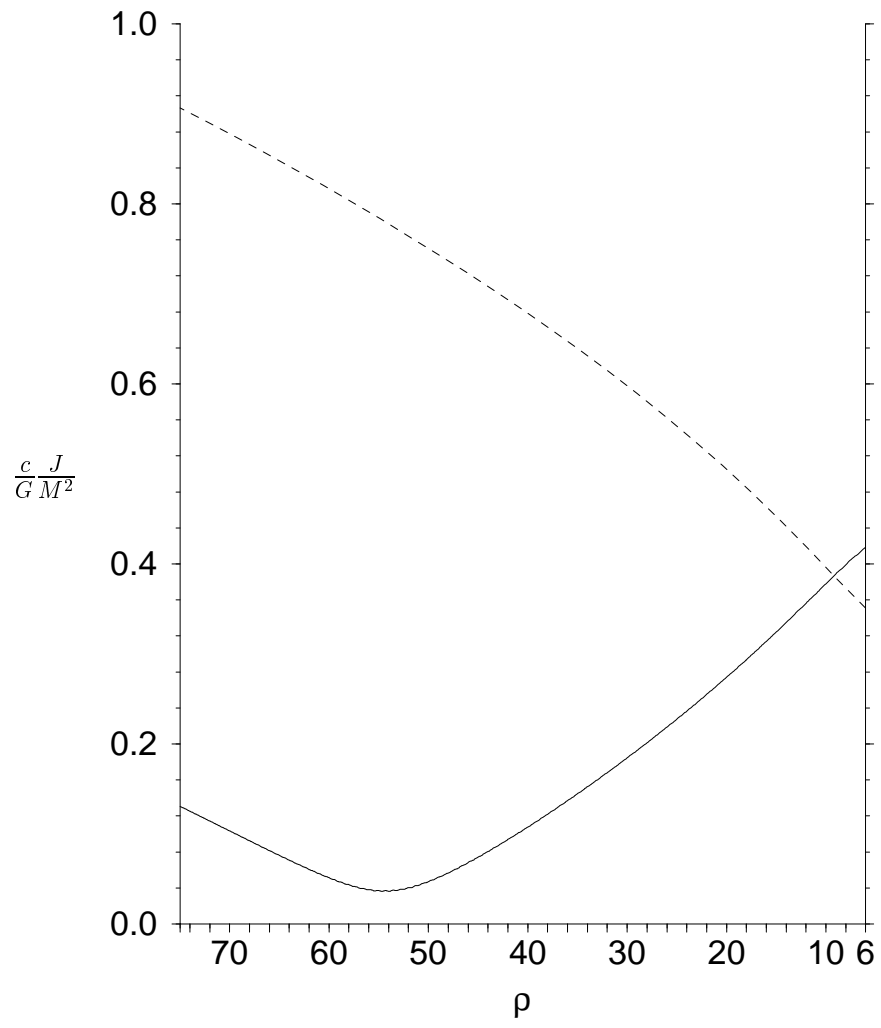


Figure 4

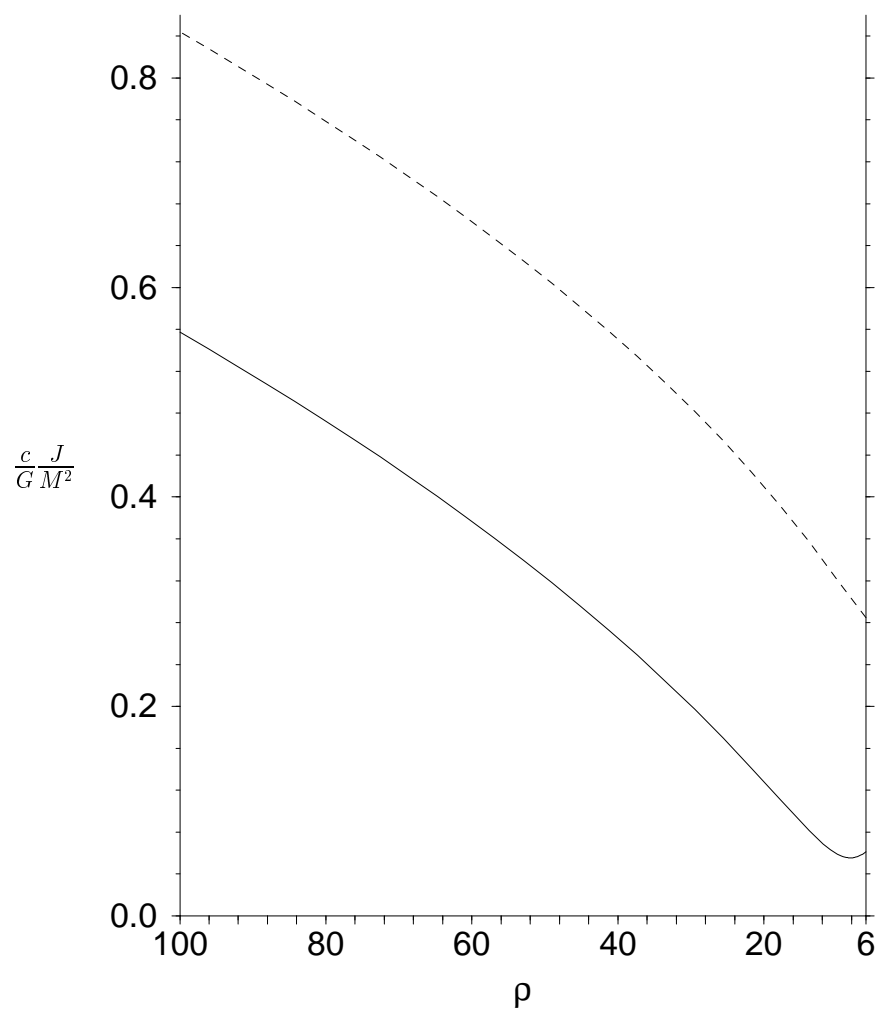


Figure 5a

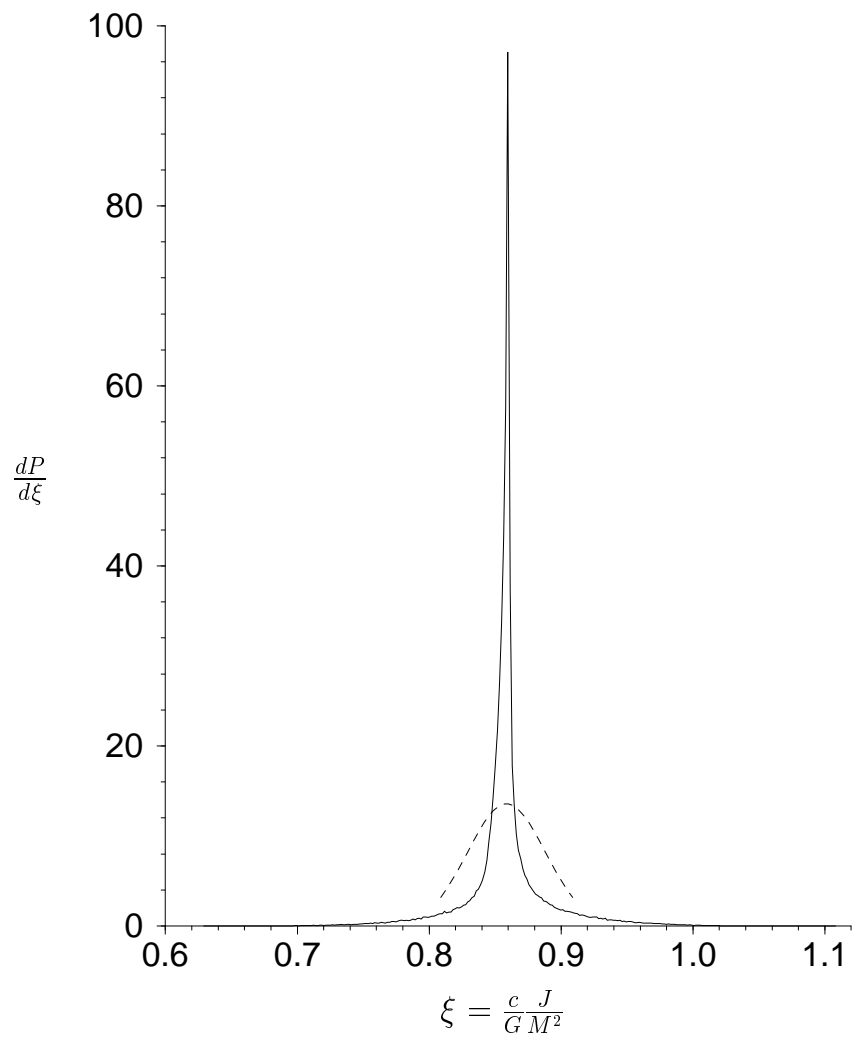


Figure 5b

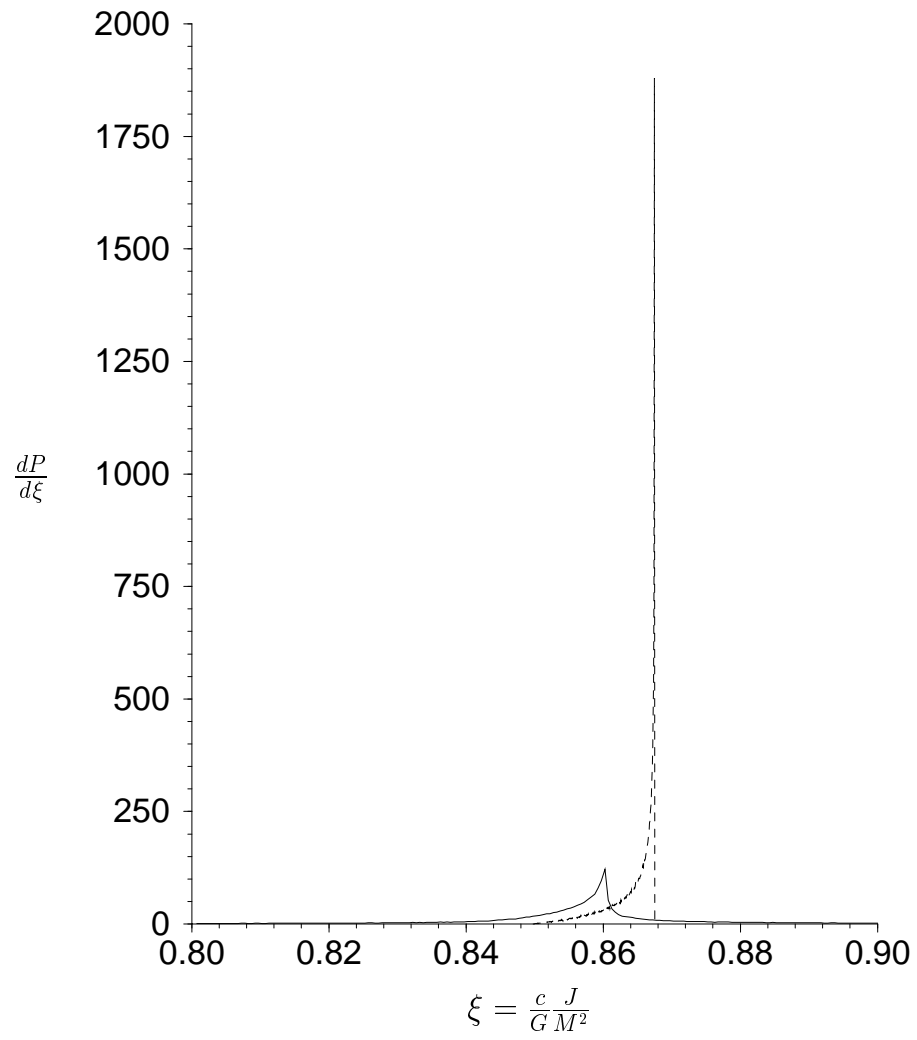




Figure 6a

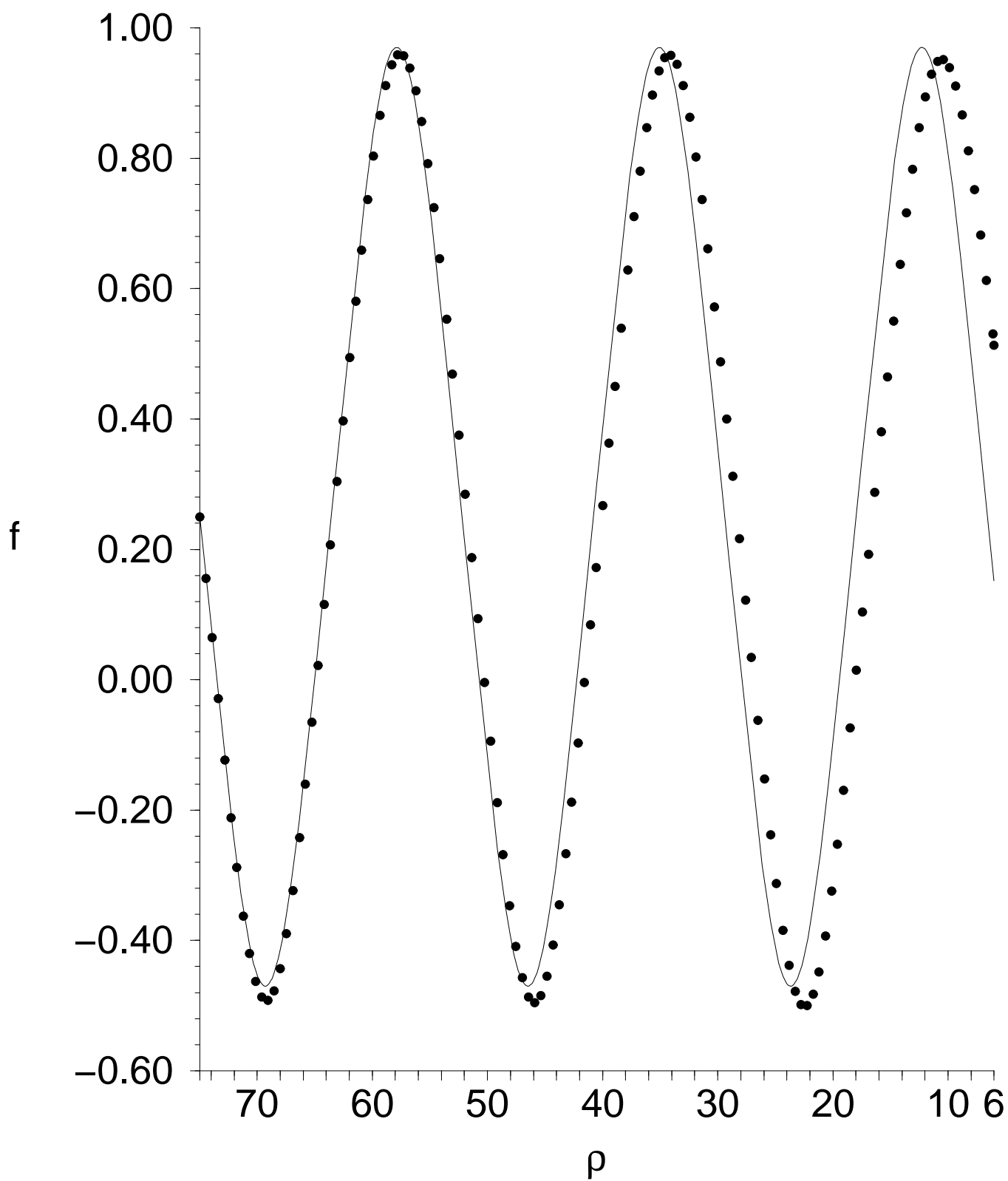


Figure 6b

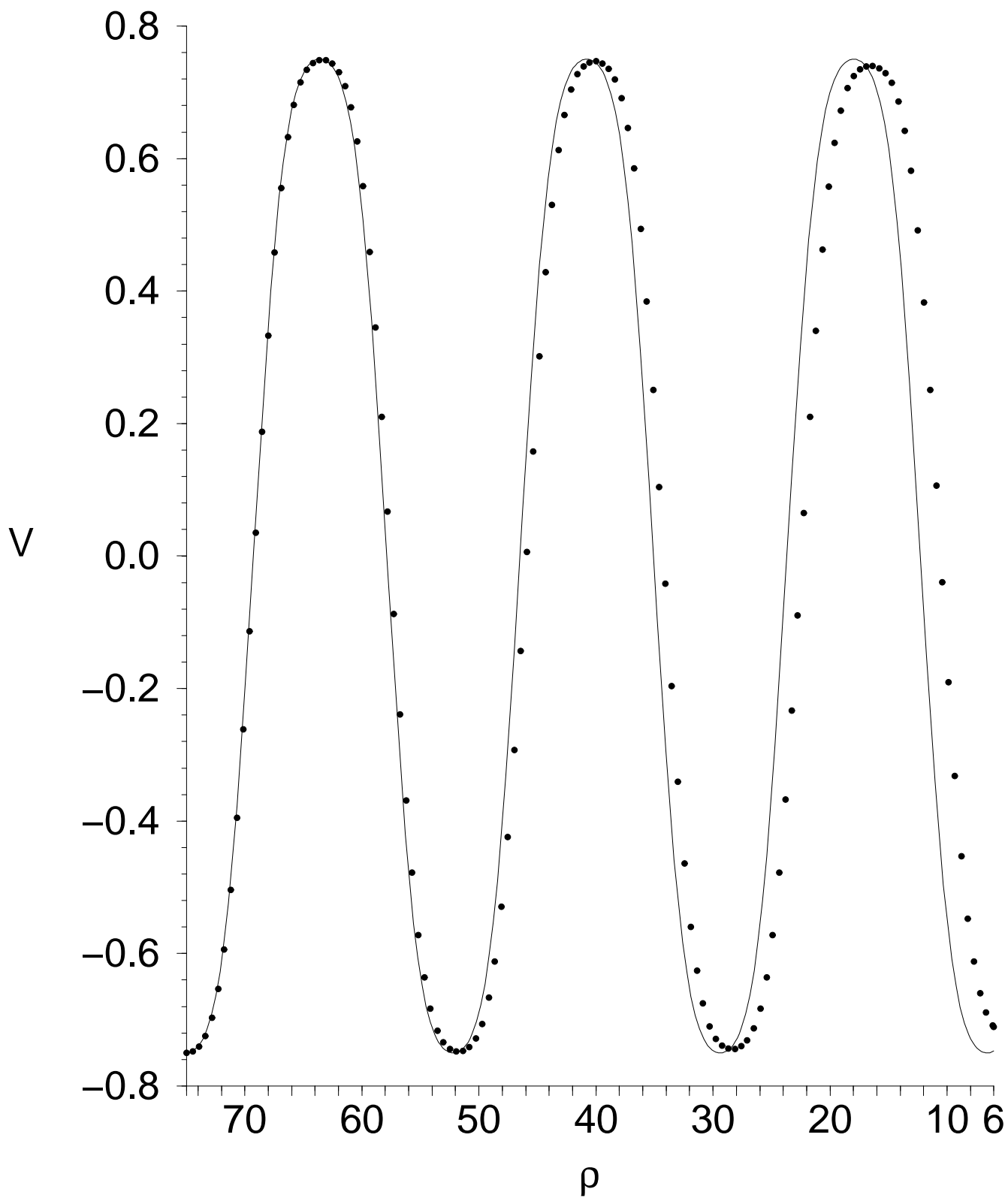


Figure 7a

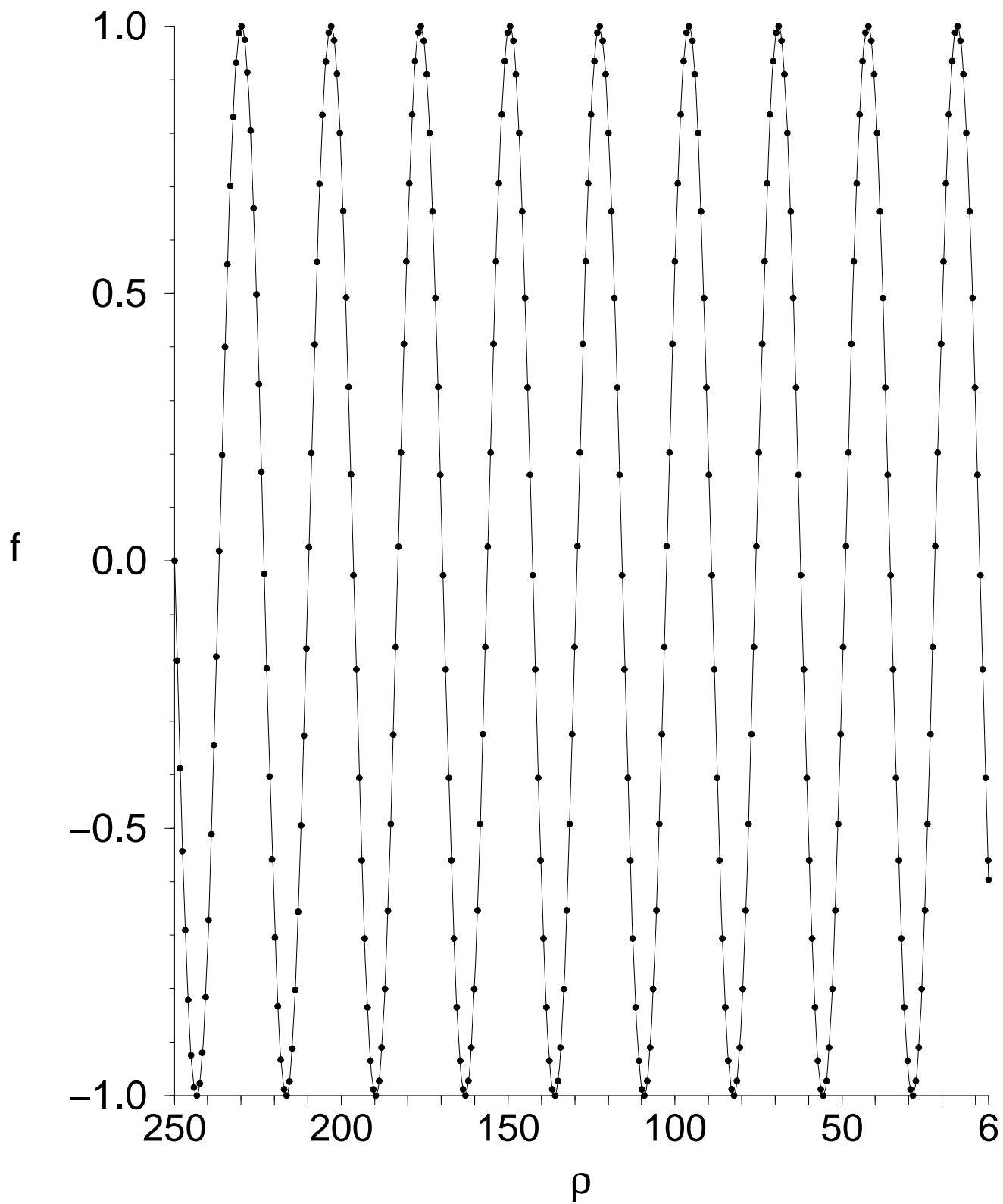


Figure 7b

